Arabian Journal of Chemistry (2017) xxx, xxx–xxx

King Saud University

Arabian Journal of Chemistry

www.ksu.edu.sa
www.sciencedirect.com

ORIGINAL ARTICLE

Solvent and substituent effect on intramolecular charge transfer in 5-arylidene-3-substituted-2,4-thiazolidinediones: Experimental and theoretical study

Milica P. Rančić [a,*], Ivana Stojiljković [a], Milena Milošević [b], Nevena Prlainović [c], Maja Jovanović [d], Miloš K. Milčić [d], Aleksandar D. Marinković [b]

[a] *Faculty of Forestry, University of Belgrade, Kneza Višeslava 1, 11030 Belgrade, Serbia*
[b] *Faculty of Technology and Metallurgy, University of Belgrade, Karnegijeva 4, 11120 Belgrade, Serbia*
[c] *Innovation Center, Faculty of Technology and Metallurgy, Karnegijeva 4, 11120 Belgrade, Serbia*
[d] *Faculty of Chemistry, University of Belgrade, Studentski trg 12-16, 11000 Belgrade, Serbia*

Received 6 September 2016; accepted 17 December 2016

KEYWORDS

Solvatochromism;
Substituent effect;
LFER;
LSER;
Quantum chemical calculation

Abstract The substituent and solvent effect on intramolecular charge transfer (ICT) in 5-arylidene-3-methyl-2,4-thiazolidinediones (series **1**) and 5-arylidene-3-phenyl-2,4-thiazolidinediones (series **2**) was studied by using experimental and theoretical methodology. The effect of specific and non-specific solvent–solute interactions on the UV–vis absorption maxima shifts was evaluated by using the Kamlet-Taft and Catalán solvent parameter sets. Linear free energy relationships (LFERs) have been applied to the UV–vis and ^{13}C NMR data by using SSP (single substituent parameter) and DSP (dual substituent parameters). Comparative LFER analysis of 10 styrenic series was performed in order to distinguish contribution of structural and electronic substituent effect on extent of π-polarization in a side chain (vinyl) group. Furthermore, the experimental findings were interpreted with the aid of *ab initio* MP2 and time-dependent density functional (TD-DFT) methods. TD-DFT calculations are performed to quantify the efficiency of intramolecular charge transfer (ICT) allowing us to define the charge-transfer distance (D_{CT}), amount of transferred charge (Q_{CT}), and difference of dipole moments between the ground and excited states (μ_{CT}). It was found that both substituents and solvents influence electron density shift, *i.e.* extent of conjugation, and affect intramolecular charge transfer character in the course of excitation.

* Corresponding author. Fax: +381 11 2547 478.
E-mail address: milica.rancic@sfb.bg.ac.rs (M.P. Rančić).
Peer review under responsibility of King Saud University.

Production and hosting by Elsevier

http://dx.doi.org/10.1016/j.arabjc.2016.12.013

Please cite this article in press as: Rančić, M.P. et al., Solvent and substituent effect on intramolecular charge transfer in 5-arylidene-3-substituted-2,4-thiazolidinediones: Experimental and theoretical study. Arabian Journal of Chemistry (2017), http://dx.doi.org/10.1016/j.arabjc.2016.12.013

1. Introduction

Thiazolidine-2,4-dione (TZD) represents an interesting scaffold responsible for numerous pharmacological properties and biological activities. TZD derivatives have attracted a significant research interest because of their synthetic diversity (Barany et al., 2005; Chen et al., 1996), and therapeutic relevance, especially since the introduction of several glitazones into clinical use for the treatment of type 2 diabetes mellitus in the late 1990s (Mendgen et al., 2012; Heidi, 2003; Casale and Stokes, 2008). Diverse chemical modifications of this heterocycle have resulted in compounds with a wide spectrum of biological activities *e.g.*, antidiabetic (Oakes et al., 1994), antiarthritic (Wiesenberg et al., 1998), antimicrobial (Tomašić et al., 2010; Tomašić and Peterlin Masic, 2009; Zvarec et al., 2012), antifungal (Sortino et al., 2007), anti-inflammatory (Ma et al., 2011; Rekha et al., 2011), anticonvulsant and antioxidant (Azam et al., 2012) activity. It has also been evidenced in numerous *in vitro* and *in vivo* studies that the TZDs have the ability to contribute to cancer therapy (Salamone et al., 2012; Kim et al., 2006). The previous research and screening a large array of TZDs against a number of enzymes showed that the ability to form interactions with a variety of biological targets is clearly not related to "unspecific" properties such as aggregation or reactivity, but rather (as could be shown by a detailed analysis of protein-ligand structures and the literature data on small molecules) to electronic and hydrogen-bonding properties (Huang et al., 2005).

Because several molecular properties, particularly electronic properties of drugs used for the treatment of diabetes mellitus correlate well with their biological activity (Maltarollo et al., 2010), future prospects for design and development of new ones can be based on the correlation between theoretical and experimental properties. Structures and relative stabilities of the potential tautomeric forms of TZD derivatives have also been extensively studied from both theoretical and experimental points of view (Lestard et al., 2015; Roux et al., 2009; Abbehausen et al., 2012; Enchev et al., 2002; Marković et al., 2004; Bharatam and Khanna, 2004). Electronic spectra of these molecules have been investigated mostly for reasons of the determination of their acidities and basicities, as well as the energies of protonation and deprotonation (Hilal and Osman, 1978; Spassova and Enchev, 2004). An *ab initio* HF and MP2 study of static hyperpolarizability of TZD has also been reported (Spassova and Enchev, 2004). In our previous research (Rančić et al., 2012), solvent and substituent effects on intramolecular charge transfer (ICT) in 5-arylidene-2,4-thiazolidine diones were investigated. The photophysical properties of TZD derivatives are mainly governed by the polarity of the medium, hydrogen bonding and electronic substituent effects at arylidene moiety (Rančić et al., 2013; Sarkar et al., 2009). One of the most important phenomena during excitation is the extent of electron transfer observed between ground and excited states. ICT usually occurs when light absorption induces a partial electronic shift from one moiety of a molecule to another, and the process strongly depends both on the bond type present between the donor and acceptor moiety (spacer) and on their intrinsic nature (Le Bahers et al., 2011). Recently, a simple approach was proposed to define a measure of the intensity of ICT excitation on the basis of the total electronic density computed for the ground and excited states (Le Bahers et al., 2011; Jacquemin et al., 2012; Ciofini et al., 2012). This procedure allows definition of ICT distance (D_{CT}) as a distance between two barycenters of the density depletion and the density increment zones, amount of transferred charge (Q_{CT}), and difference of dipole moments between the ground and excited states (μ_{CT}).

Two series of 5-arylidene-3-methyl-2,4-thiazolidinediones (series **1**) and 5-arylidene-3-phenyl-2,4-thiazolidinediones (series **2**) (Scheme 1) were synthesized in this work. The contribution of the solvent–solute interactions on the shifts in UV spectra was investigated by the use of linear solvation energy relationships (LSER). The effects of solvent dipolarity/-polarizability and solvent–solute hydrogen bonding interactions were evaluated by means of the LSER model of Kamlet-Taft (Kamlet et al., 1981), given by Eq. (1):

$$\nu_{max} = h + s\pi^* + b\beta + a\alpha \quad (1)$$

where ν_{max} is the absorption maxima shifts, π^* is an index of the solvent dipolarity/-polarizability; β is a measure of the solvent hydrogen-bond acceptor (HBA) basicity; α is a measure of the solvent hydrogen-bond donor (HBD) acidity, and h is the regression value in cyclohexane as reference solvent. The solvent parameters used in Eq. (1) are given in Table S1. The regression coefficients s, b and a in Eq. (1) measure the relative susceptibilities of the absorption frequencies to the solvent effect.

The effects of solvent dipolarity, polarizability and solvent–solute hydrogen bonding interactions were evaluated by means of the linear solvation energy relationship (LSER) model of Catalán (Catalán, 2009), given by Eq. (2):

$$\nu_{max} = h + a\mathrm{SA} + b\mathrm{SB} + c\mathrm{SP} + d\mathrm{SdP} \quad (2)$$

where SA, SB, SP and SdP characterize solvent acidity, basicity, polarizability and dipolarity of a solvent, respectively; and a to d are the regression coefficients describing the sensitivity of the absorption maxima to the different types of the solvent–solute interactions. The solvent parameters used in Eq. (2) are given in Table S2. Separation of non-specific solvent effects, term π^* in Eq. (1), into two terms: dipolarity and polarizability, SP and SdP in Eq. (2), contributes to advantageous analysis of the solvatochromism of studied compounds.

Except for LSER methodology, the linear free energy relationship (LFER) principles were applied to get an insight into factors influencing ^{13}C NMR substituent induced chemical shifts, *SCS*, or ν_{max} of the studied compounds. The transmission of electronic substituent effects (Scheme 1) was analyzed by using the Hammett or single substituent parameter equation (SSP) in the form given by Eq. (3):

$$Y = \rho\sigma + h \quad (3)$$

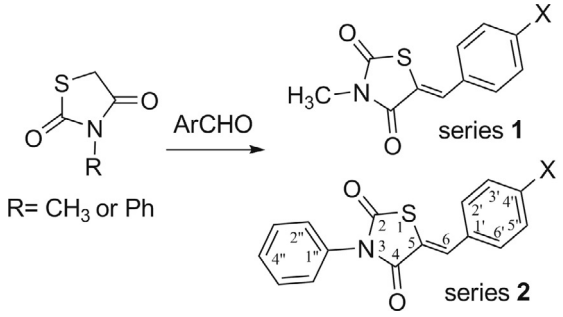

X	series 1	series 2
H	**1a**	**2a**
CH_3	**1b**	**2b**
OCH_3	**1c**	**2c**
Br	**1d**	**2d**
Cl	**1e**	**2e**
F	**1f**	**2f**
$N(CH_3)_2$	**1g**	**2g**
NO_2	**1h**	**2h**
3,4-di-OCH_3	**1i**	**2i**

Scheme 1 Syntheses and structures of 3-substituted-5-arylidene-2,4-thiazolidinediones.

where Y is a substituent–dependent value: v_{max} or *SCS*, is the proportionality constant reflecting the sensitivity of the v_{max} to the substituent effects, σ is the corresponding substituent constant, and h is the intercept (*i.e.* describes the unsubstituted member of the series) (Hansch et al., 1995). The values (Table S3) correspond to an additive blend of polar and -delocalization effects. In order to separate substituent electronic effects into polar (inductive/filed) and resonance component, the further analysis of *SCS* is based on LFER principle by using the dual-substituent parameter model (DSP) Eq. (4):

$$Y = \rho_F \sigma_F + \rho_R \sigma_R + h \quad (4)$$

where Y are substituent-dependent values *SCS*, ρ_F and ρ_R are the proportionality constants, reflecting the sensitivity of ^{13}C NMR chemical shifts to substituent field and resonance effect, σ represents the corresponding substituent constant, and h is the intercept. In DSP equation, Y values are correlated by a linear combination of substituent field, σ_F, and resonance, σ_R, effect. The calculated values: ρ, ρ_F, and ρ_R are relative measures of the extent of the transmission of overall, polar (inductive/field) and resonance effects through the investigated system, respectively. Even in those cases where a good correlation with Eq. (3) is obtained, use of Eq. (4) gives more detailed information about the mode of transmission of substituent effects. Chemical properties of series **1** and **2** (Scheme 1) have been comparatively investigated by using experimental and theoretical methods. The computational studies include MP2 geometry optimization, NMR chemical shift determination and Time-dependent density functional theory (TD-DFT) calculations of absorption spectra, electronic transition and evaluation of ICT in the course of transition.

2. Experimental

2.1. Materials

Details on materials are given in Supplementary material.

2.2. Synthesis of 2,4-thiazolidinedione, 3-methyl-2,4-thiazolidinedione, diphenylthiourea and 3-phenyl-2,4-thiazolidinedione

Details related to syntheses of 2,4-thiazolidinedione (Jain et al., 2009; Brown, 1961), 3-methyl-2,4-thiazolidinedione (Macháček et al., 1981), diphenylthiourea (Yamin and Yusof, 2003) and 3-phenyl-2,4-thiazolidinedione (Singh et al., 1981) are given in Supplementary material.

2.3. Synthesis of 5-arylidene-3-substituted-2,4-thiazolidinedione

Two series of 5-arylidene-3-methyl-2,4-thiazolidinediones (series **1**) and 5-arylidene-3-phenyl-2,4-thiazolidinediones (series **2**) were synthesized by the Knoevenagel condensation of corresponding 3-methyl- or 3-phenyl-2,4-thiazolidinediones with the appropriate aryl aldehydes (Rančić et al., 2012).

2.4. Characterization methods

Full details of characterization methods are given in Supplementary material.

2.5. Theoretical calculations

Methods used for theoretical calculation are given in Supplementary material.

2.6. Results of the characterization of series 1 and series 2

^1H and ^{13}C NMR, FTIR and elemental analysis data of known compounds **1a–c, 1h, 2a–c, 2h** and **2i** are given in Supplementary material, while data of newly synthesized compounds are given in detail:

5-benzylidene-3-methyl-2,4-thiazolidinedione (1a). White solid; Yield: 79%, Melting point (m.p.): 130–131 °C (lit. m.p. 133 °C (Yang et al., 2005));

5-(4-methylbenzylidene)-3-methyl-2,4-thiazolidinedione (1b). White solid; Yield: 73%, m.p.: 148–150 °C (lit. m.p. 125–127 °C (Chandrappa et al., 2008));

5-(4-methoxybenzylidene)-3-methyl-2,4-thiazolidinedione (1c). Yellow solid; Yield: 88%, m.p.: 148–150 °C (lit. m.p. 145–147 °C (Yang et al., 2005));

5-(4-bromobenzylidene)-3-methyl-2,4-thiazolidinedione (1d). Yellow solid; Yield: 82%, m.p.: 162–166 °C; ^1H NMR: 3.1 (3H, s, C**H**$_3$); 7.5–7.7 (4H, dd, Ph); 7.9 (1H, s,=C**H**—); ^{13}C NMR: 28.1 (**C**H$_3$, N-CH$_3$); 115.8 (**C5**, TZD); 123.4 (**C4′,** Ph); 128.1; 128.2 (**C2′**, **C6′,** Ph); 132.5; 133.0 (**C3′**, **C5′,** Ph); 130.4 (**C6**, =CH—**);** 134.5 (**C1′**, Ph); 165.8 (**C4**, 4-C=O); 166.4 (**C2**, 2-C=O); IR (KBr, cm^{-1}): 3023 (C—H stretching of phenyl group); 1736 (C=O stretching); 1682 (amide band I – C2=O and C4=O stretching); Elemental Analysis:

Calculated: %C, 44.31; %H, 2.70; %Br, 26.80; %N, 4.70; %O, 10.73; %S, 10.75.

Found: %C, 44.27; %H, 2.73; %Br, 26.75; %N, 4.74; %O, 10.70; %S, 10.81.

5-(4-chlorobenzylidene)-3-methyl-2,4-thiazolidinedione (1e). Yellow solid; Yield: 89%, Melting point: 171–172 °C; ^1H NMR: 3.2 (3H, s, N-C**H**$_3$); 7.3 (2H, d, Ph); 7.8 (1H, s, =C**H**—); 7.4 (2H, d, Ph); ^{13}C NMR: 28.0 (**C**H$_3$, N-CH$_3$); 129.5 (**C3′**, **C5′**, Ph); 131.3 (**C2′**, **C6′**, Ph); 122.1 (**C5**, TZD); 136.6 (**C6**, =CH—**);** 131.6 (**C1′**, Ph); 132.2 (**C4′**, Ph); 166.2 (**C4**, 4-C=O); 167.4 (**C2**, 2-C=O); IR (KBr, cm^{-1}): 3021 (C—H stretching of phenyl group); 1737 (C=O stretching); 1685 (amide band I – C2=O and C4=O stretching); Elemental Analysis:

Calculated: %C, 52.08; %H, 3.18; %Cl, 13.97; %N, 5.52; %O, 12.61; %S, 12.64.

Found: %C, 51.73; %H, 3.21; %Cl, 14.04; %N, 5.60; %O, 12.70; %S, 12.72.

5-(4-fluorobenzylidene)-3-methyl-2,4-thiazolidinedione (1f). Yellow solid; Yield: 85%; m.p.: 170–171 °C; ^1H NMR: 3.1 (3H, s, C**H**$_3$); 7.3–7.4 (2H, m, Ph); 7.6–7.7 (2H, m, Ph); 7.9 (1H, s, =C**H**—); ^{13}C NMR: 28.1 (**C**H$_3$, N-CH$_3$); 115.6 (**C5**, TZD); 116.6; 117.0 (**C3′**, **C5′,** Ph); 131.4 (**C6,** =CH—**);** 131.7 (**C1′**, Ph); 132.7; 132.9 (**C2′**, **C6′**, Ph); 160.7 (**C4′**, Ph); 165.7 (**C4**, 4-C=O); 166.0 (**C2**, 2-C=O); IR (KBr, cm^{-1}): 3024 (C—H stretching of phenyl group); 1741 (C=O stretching); 1690 (amide band I – C2=O and C4=O stretching); Elemental Analysis:

Calculated: %C, 55.69; %H, 3.40; %F, 8.01; %N, 5.90; %O, 13.49; %S, 13.52.

Found: %C, 55.70; %H, 3.37; %F, 7.97; %N, 5.93; %O, 13.51; %S, 13.52.

Please cite this article in press as: Rančić, M.P. et al., Solvent and substituent effect on intramolecular charge transfer in 5-arylidene-3-substituted-2,4-thiazolidinediones: Experimental and theoretical study. Arabian Journal of Chemistry (2017), http://dx.doi.org/10.1016/j.arabjc.2016.12.013

5-(4-dimethylaminobenzylidene)-3-methyl-2,4-thiazolidine dione (1g). Orange solid; Yield: 92%, m.p.: 170–173 °C; ^{1}H NMR: 3.0 (3H, s, N-C**H**$_3$); 3.1 (6H, s, C**H**$_3$); 7.3–7.4 (2H, m, Ph); 6.8–6.9 (2H, m, Ph); 7.8 (1H, s, =C**H**—); ^{13}C NMR: 27.8 (**C**H$_3$, N-CH$_3$); 39.8 (**C**H$_3$, N(CH$_3$)$_2$); 112.3; 117.0 (**C3′**, **C5′**, Ph); 113.7 (**C5**, TZD); 120.0 (**C1′**, Ph), 132.5 (**C2′**, **C6′**, Ph); 134.0 (**C6**, =CH—); 151.8 (**C4′**, Ph); 166.3 (**C4**, 4-C=O); 172.6 (**C2**, 2-C=O); IR (KBr, cm^{-1}): 3007 (C—H stretching of phenyl group); 1732 (C=O stretching); 1672 (amide band I – C2=O and C4=O stretching); Elemental Analysis:

Calculated: %C, 59.52; %H, 5.38; %N, 10.68; %O, 12.20; %S, 12.22.

Found: %C, 59.49; %H, 5.36; %N, 10.73; %O, 12.19; %S, 12.23.

5-(4-nitrobenzylidene)-3-methyl-2,4-thiazolidinedione (1h). Yellow solid; Yield: 75%, m.p.: 220–222 °C (lit m.p. 222–224 °C (Romagnoli et al., 2013));

5-(3,4-dimetoxybenzylidene)-3-methyl-2,4-thiazolidinedione (1i). Yellow solid; Yield: 91%, m.p.: 172–175 °C; ^{1}H NMR: 3.3 (3H, s, N-C**H**$_3$); 3.5 (3H, s, OCH$_3$); 3.6 (3H, s, OCH$_3$) 7.2 (H, d, CH (C$_2'$)); 7.4 (H, d, CH(C3′)); 7.4 (H, d, CH (C6′)); 8.1 (1H, s, =C**H**—); ^{13}C NMR: 27.8 (**C**H$_3$, N-CH$_3$); 55.9, 56.1 (**C**H$_3$, OCH$_3$); 111.3 (**C3′**, **C5′**, Ph); 122.6 (**C2′**, **C6′**, Ph); 112.3 (**C5**, TZD); 148.6 (**C6**, =CH-); 126.0 (**C1′**, Ph); 149.2 (**C4′**, Ph); 166.4 (**C4**, 4-C=O); 177.6 (**C2**, 2-C=O); IR (KBr, cm^{-1}): 3019 (C—H stretching of phenyl group); 1735 (C=O stretching); 1683 (amide band I – C2=O i C4=O stretching); Elemental Analysis:

Calculated: %C, 55.90; %H, 4.69; %N, 5.01; %O, 22.91; %S, 11.48.

Found: %C, 56.00; %H, 4.64; %N, 5.00; %O, 22.89; %S, 11.47.

5-benzylidene-3-phenyl-2,4-thiazolidinedione (2a). White solid; Yield: 89%, m.p.: 209–209.8 °C (lit m.p. 208–209 °C (Yang et al., 2008));

5-(4-methylbenzylidene)-3-phenyl-2,4-thiazolidinedione (2b). Yellow solid; Yield: 80%, m.p.: 190–191 °C (lit m.p. 190–191 °C (Yang et al., 2008));

5-(4-methoxybenzylidene)-3-phenyl-2,4-thiazolidinedione (2c). White solid; Yield: 79%, m.p.: 199–201 °C (lit m.p. 200–202 °C (Yang et al., 2008));

5-(4-bromobenzylidene)-3-phenyl-2,4-thiazolidinedione (2d). Yellow solid; Yield: 78%, m.p.: 211–215.5 °C; ^{1}H NMR: 7.0 (H, s, N-Ph); 7.3–7.4 (4H, m, Ph), 7.5–7.6 (4H, m, Ph), 7.8 (1H, s, =C**H**—); ^{13}C NMR: 121.0 (**C5,** TZD); 122.1 (**C4′**, Ph), 128 (**C2″**, **C4″**, **C6″**, N-Ph); 129.2 (**C2′, C6′**, Ph, **C3″**, **C5″**, N-Ph); 130.1 (**C2′**, **C6′**, Ph); 131.3 (**C1″**, N-Ph); 131.3 (**C3′**, **C5′**, Ph); 132.6 (**C1′**, Ph); 134.6 (**C6**, =CH—); 163.4 (**C4**, 4-C=O); 166.2 (**C2**, 2-C=O); IR (KBr, cm^{-1}): 3033 (C—H stretching of phenyl group); 1716 (C=O stretching); 1644 (amide band I – C2=O i C4=O stretching); Elemental Analysis:

Calculated: %C, 53.35; %H, 2.80; %Br, 22.18; %N, 3.89; %O, 8.88; %S, 8.90.

Found: %C, 53.34; %H, 2.78; %Br, 22.20; %N, 3.87; %O, 8.90; %S, 8.91.

5-(4-chlorobenzylidene)-3-phenyl-2,4-thiazolidinedione (2e). Yellow solid; Yield: 81%, m.p.: 203–204 °C; ^{1}H NMR: 7.3 (H, s, N-Ph); 7.5 (4H, m, N-Ph); 7.5 (2H, m, Ph); 7.6 (2H, m, Ph); 7.9 (1H, s, =C**H**—); ^{13}C NMR: 121.7 (**C5,** TZD); 127.2 (**C2″**, **C4″**, **C6″,** N-Ph); 129.4 (**C3′**, **C5′**, Ph); 129.6 (**C3″**, **C5″**, N-Ph); 130.1 (**C4′**, Ph); 131.4 (**C2′**, **C6′**, Ph); 131.7 (**C1″**, N-Ph); 133.0 (**C1′**, Ph), 136.8 (**C6**, =CH—); 165.5 (**C4**, 4-C=O); 166.8 (**C2**, 2-C=O); IR (KBr, cm^{-1}): 3020 (C—H stretching of phenyl group); 1738 (C=O stretching); 1696 (amide band I – C2=O i C4=O stretching); Elemental Analysis:

Calculated: %C, 60.86; %H, 3.19; %Cl, 11.23; %N, 4.44; %O, 10.13; %S, 10.15.

Found: %C, 60.88; %H, 3.20; %Cl, 11.21; %N, 4.47; %O, 10.09; %S, 10.15.

5-(4-fluorobenzylidene)-3-phenyl-2,4-thiazolidinedione (2f). Yellow solid; Yield: 82%, m.p.: 165–166 °C; ^{1}H NMR: 7.0 (H, s, N-Ph); 7.1 (4H, m, N-Ph); 7.5 (4H, m, Ph); 7.8 (H, s, =C**H**—); ^{13}C NMR: 120.82 (**C3′**, **C5′**, Ph); 120.98 (**C5,** TZD); 124.60 (**C2″**, **C4″**, **C6″,** N-Ph); 127.9 (**C3″**, **C5″**, N-Ph); 129.0 (**C2′**, **C6′**, Ph); 120.6 (**C1′,** Ph); 129.3 (**C1″**, N-Ph); 136.5 (**C6**, =CH—); 154.9 (**C4′**, Ph); 169.7 (**C4**, 2-C=O); 171.4 (**C2**, 2-C=O); IR (KBr, cm^{-1}): 3052 (C—H stretching of phenyl group); 1723 (C=O stretching); 1637 (amide band I – C2=O i C4=O stretching); Elemental Analysis:

Calculated: %C, 64.20; %H, 3.37; %F, 6.35; %N, 4.68; %O, 10.69; %S, 10.71.

Found: %C, 64.13; %H, 3.40; %F, 6.34; %N, 4.71; %O, 10.70; %S, 10.72.

5-(4-dimethylaminobenzylidene)-3-phenyl-2,4-thiazolidine dione (2g). Yellow solid; Yield: 85%, m.p.: 239–240 °C; ^{1}H NMR: 3.1 (6H, s, N(C**H**$_3$)$_2$); 6.7 (2H, d, Ph); 7.3 (1H, s, N-Ph); 7.3 (2H, d, Ph); 7.5 (4H, m, N-Ph); 7.9 (1H, s, =C**H**—); ^{13}C NMR: 39.9 (**C**H$_3$, N(CH$_3$)$_2$); 111.9 (**C3′**, **C5′**, Ph); 120.6, 113.7 (**C5**, TZD); 127.4 (**C1′**, Ph); 129.3 (**C2″**, **C4″**, **C6″**, N-Ph); 132.6 (**C3″**, **C5″**, N-Ph); 135.5 (**C2′**, **C6′**, Ph); 136.5 (**C6**, =CH—); 185.4 (**C1″**, N-Ph); 147.8 (**C4′**, Ph); 151.6 (**C4′**, Ph); 165.6 (**C4**, 4-C=O); 166.2 (**C2**, 2-C=O); IR (KBr, cm^{-1}): 3066 (C—H stretching of phenyl group); 1735 (C=O stretching); 1686 (amide band I – C2=O i C4=O stretching); Elemental Analysis:

Calculated: %C, 66.64; %H, 4.97; %N, 8.64; %O, 9.86; %S, 9.88.

Found: %C, 66.61; %H, 5.00; %N, 8.65; %O, 9.89; %S, 9.85.

5-(4-nitrobenzylidene)-3-phenyl-2,4-thiazolidinedione (2h). Orange solid; Yield: 80%, m.p.: 249–250 °C (lit m.p. 238–240 °C (Yang et al., 2008));

5-(3,4-dimetoxybenzylidene)-3-phenyl-2,4-thiazolidinedione (2i). Yellow solid; Yield: 85%, m.p.: 208–209 °C (lit m.p. 209–210 °C (Yang et al., 2008));

3. Results and discussion

3.1. Spectral properties of 5-arylidene-3-substituted-2,4-thiazolidinediones

It is well known that spectral behavior of molecule, *i.e.* position, intensity and shape of absorption band, depends on the properties of solvent used. Indeed, a change of solvent is accompanied by a variation of dipolarity/polarizability and hydrogen bonding intermolecular solvent-solute interactions, which means that the study of the solvent effects on the absorption spectra allows assessment of fundamental molecular properties (Reichardt, 2003). A generally accepted concept,

Please cite this article in press as: Rančić, M.P. et al., Solvent and substituent effect on intramolecular charge transfer in 5-arylidene-3-substituted-2,4-thiazolidinediones: Experimental and theoretical study. Arabian Journal of Chemistry (2017), http://dx.doi.org/10.1016/j.arabjc.2016.12.013

concerning the relationship between molecular structure and shift in absorption spectrum, explains that more planar structure supports higher contribution of extended π-electron delocalization which is reflected in bathochromic shift. Based on this, two series of TZDs coupled with substituted benzaldehydes were synthesized, supposing that the obtained π-conjugated systems could show different sensitivities toward solvent and substituent effects. The exocyclic double bond takes *Z*-configuration, as it was evidenced by higher stability of these isomers (Section 3.3). Two factors could have favorable effect: lower crowdedness and appropriate contribution of intramolecular hydrogen bonding which could exist between C6-H hydrogen and C4═O oxygen (Fig. S1) (Luo et al., 2010).

The absorption spectra of the investigated compounds were recorded in nineteen solvents of different properties, and the characteristic spectra are shown in Fig. 1. Two absorbance bands at 250–280 nm and at 320–380 nm, corresponding to π–π^* and n–π^* (Rančić et al., 2012) transitions, respectively, were distinctly observed. From the presented UV–vis spectra (Fig. 1), a diversity of the spectra could be noticed, and broad band at higher wavelength originates from n–π^* transitions. The data from Tables 1 and 2 indicate that values of absorption frequencies, ν_{max}, depend on substituent and solvent effect, though the absorption bands of both electron-donor and electron-acceptor substituted derivatives appear at similar wavelengths (in the range 10–20 nm). The absorption maxima of 5-arylidene-3-methyl-2,4-thiazolidinediones showed bathochromic shift compared to parent compound in most solvents (except **1f** in 2-PrOH, 2ME, 2CE, Et_2O and Pen, and **1g** in 2CE; abbreviations are given in Table 1). The introduction of electron-donor substituents produces larger bathochromic shifts suggesting a more pronounced ICT. Low absorption band at ~400 nm, observed for **1f** in AcN, could originate from photoisomeration of more stable *Z*- to *E*-isomer (Uchiyama et al., 2003). On the other hand, absorption maxima of 5-arylidene-3-phenyl-2,4-thiazolidinedione showed red shift for all substances, and the largest one was found for *dimethylamino* derivatives, *i.e.* **1g** and **2g**.

3.2. Solvent effects on the UV–Vis absorption spectra: Correlation with multi-parameter solvent polarity scales (LSER analysis)

The effect of various types of solvent–solute interactions on the absorption maxima shifts was interpreted by means of Kamlet-Taft and Catalán LSER models. The correlation analysis was carried out using Microsoft Excel software at confidence level of 95%. The goodness of fit is discussed using the correlation coefficient (*R*), the standard error of the

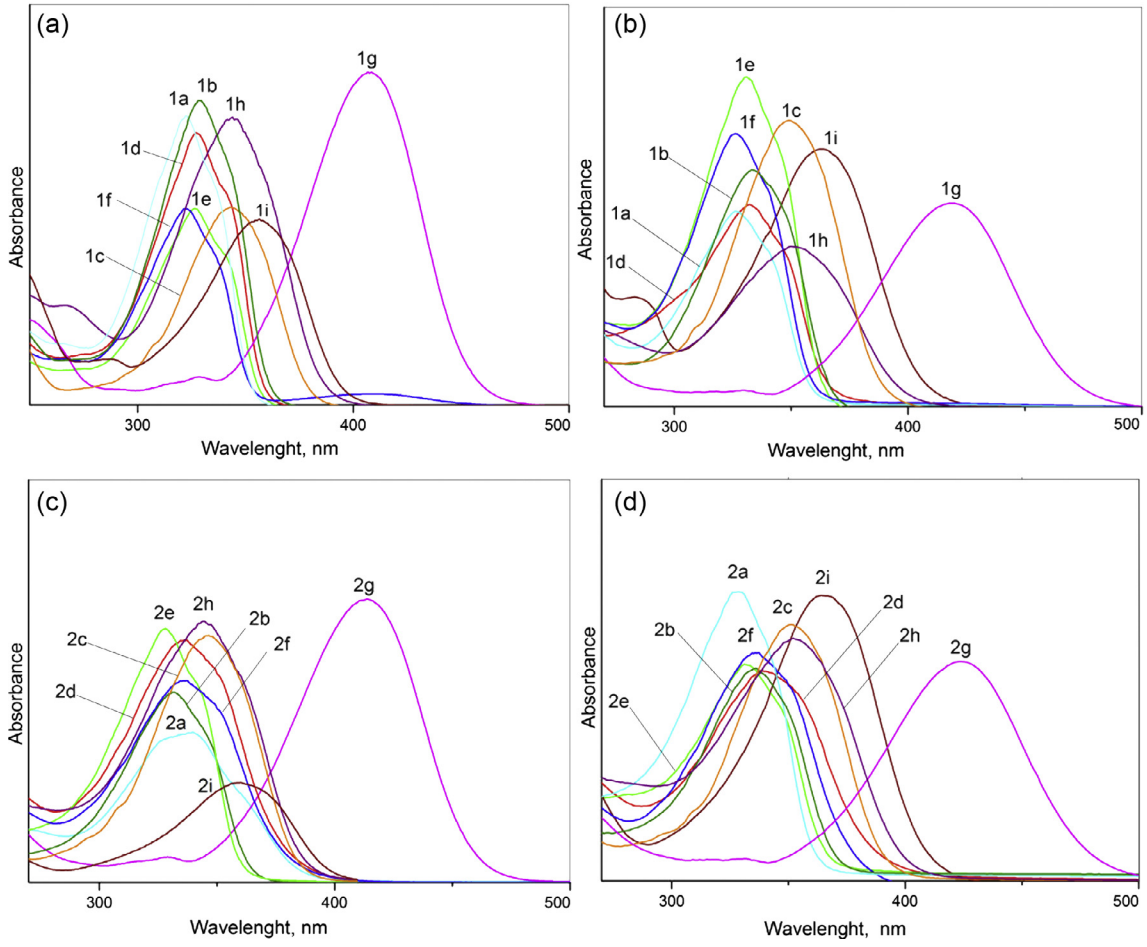

Figure 1 Absorption spectra of compounds **1a**–**1i** in acetonitrile (a) and DMSO (b), and compounds **2a**–**2i** in acetonitrile (c) and DMSO (b).

Table 1 Absorption frequencies of series **1** in selected solvents.

Solvent/compound	$\nu_{max} \times 10^{-3}$ (cm^{-1})								
	1a	**1b**	**1c**	**1d**	**1e**	**1f**	**1g**	**1h**	**1i**
Ethanol (EtOH)	30.95	29.91	29.51	30.77	30.06	30.63	23.67	28.52	28.59
Methanol (MeOH)	30.66	30.14	29.33	30.23	30.00	30.53	24.03	28.62	29.64
1-Propanol (1-PrOH)	30.69	29.67	29.59	30.34	30.46	30.50	26.63	29.51	29.46
2-Propanol (2-PrOH)	30.34	29.67	29.67	30.40	30.29	30.53	24.30	29.29	28.96
1-Butanol (1-BuOH)	30.58	30.06	29.30	29.98	30.20	30.53	24.32	29.03	28.32
2-Methylpropan-1-ol (i-BuOH)	30.50	30.22	29.47	30.24	29.89	30.58	24.23	28.96	28.93
2-Metoxyethanol (2ME)	30.47	29.51	29.46	30.41	30.46	30.79	26.20	29.19	29.78
2-Chloroethanol (2CE)	29.84	29.51	29.51	29.62	29.73	30.06	23.27	28.37	29.26
Diethyl ether (Et_2O)	30.64	30.45	29.44	30.28	30.56	30.77	25.74	29.14	29.68
Diisopropyl ether (iPr_2O)	30.86	30.49	29.15	30.49	30.77	30.86	25.03	29.41	29.17
Cyclohexane (Ch)	30.83	30.50	29.42	30.26	30.37	30.86	25.87	29.11	30.30
Heptane (Hp)	30.87	30.34	29.40	30.40	30.46	30.93	25.99	29.40	29.82
Pentane (Pen)	30.87	30.50	29.44	30.40	30.53	30.98	26.20	29.41	29.90
trans-1,2-Dichloroethylene (1,2-DCE)	30.50	29.91	28.92	30.12	30.07	30.42	24.64	29.36	29.04
Dioxane	29.80	29.03	28.27	29.51	29.67	29.95	23.95	27.88	28.20
Acetonitrile (AcN)	31.43	30.65	29.46	30.55	30.68	30.87	25.27	29.86	29.51
N,*N*-Dimethylformamide (DMF)	30.30	30.00	29.70	30.19	30.19	30.63	23.76	28.42	29.66
Dimethyl sulfoxide (DMSO)	30.34	30.12	29.78	29.50	30.15	30.58	24.33	28.42	29.43
Formamide (FA)	30.17	29.67	29.28	30.24	29.59	30.05	23.43	28.05	29.89

Table 2 Absorption frequencies of series **2** in selected solvents.

Solvent/compound	$\nu_{max} \times 10^{-3}$ (cm^{-1})								
	2a	**2b**	**2c**	**2d**	**2e**	**2f**	**2g**	**2h**	**2i**
Ethanol	30.82	30.17	28.82	30.35	30.77	30.49	23.98	29.11	29.78
Methanol	30.96	30.30	29.03	30.44	30.96	30.58	24.21	29.24	29.86
1-Propanol	30.96	30.26	28.99	30.49	30.91	30.53	24.36	29.15	29.94
2-Propanol	30.91	30.35	28.94	30.44	30.90	30.53	24.30	29.33	28.66
1-Butanol	30.86	30.12	28.94	30.44	30.86	30.49	24.30	29.15	29.89
2-Methylpropan-1-ol	30.86	30.26	28.78	30.35	30.82	30.44	24.30	29.24	29.93
2-Metoxyethanol	30.82	30.17	28.69	30.40	30.80	30.26	24.01	28.78	29.78
2-Chloroethanol	30.49	29.81	28.41	30.03	30.43	30.17	23.82	28.69	29.55
Diethyl ether	30.96	30.58	29.28	30.58	30.90	30.67	25.03	29.33	30.25
Diisopropyl ether	30.86	30.49	29.15	30.49	30.86	30.77	25.03	29.41	30.17
Cyclohexane	31.01	30.44	29.37	30.49	30.96	30.49	24.24	29.28	29.72
Heptane	29.99	29.41	29.46	29.45	29.90	29.41	25.06	28.33	29.36
Pentane	30.03	29.50	29.46	29.37	30.01	29.50	25.22	29.46	29.53
trans-1,2-Dichloroethylene	30.67	30.12	28.99	30.12	30.58	30.26	24.72	29.03	29.09
Dioxane	30.03	29.41	28.29	29.33	29.90	29.56	24.21	28.17	29.36
Acetonitrile	30.70	30.11	29.11	29.95	30.37	30.27	24.93	28.41	27.85
N,*N*-Dimethylformamide	30.84	30.03	28.70	29.60	30.29	29.96	23.91	28.63	27.63
Dimethyl sulfoxide	30.65	29.83	28.40	29.45	30.14	29.38	23.63	28.36	27.38
Formamide	30.22	29.49	28.14	29.00	29.81	29.17	23.21	28.46	27.34

estimate (*sd*), and Fisher's significance test (*F*). The regression values *h*, *s*, *a*, and *b* (Kamlet-Taft), and *c*, *d*, *a*, and *b* (Catalán) fit are given in Tables 3–6, respectively.

Presented results indicate that the solvent effects on UV–Vis spectra are complex due to diversity of contribution of both solvent and substituent effects. It can be noticed, from the results given in Tables 3 and 4, that in most cases non-specific solvent effect is a factor of the highest contribution to UV–vis spectral shifts. The negative sign of coefficient *s* for most compounds, except coefficient *s* for **2a** and **2b** (Table 4), and *a* coefficient for all studied compounds, indicates bathochromic (red) shift with increasing solvent dipolarity/polarizability and hydrogen-bond donating capability. This suggests better stabilization of the electronic excited state relative to ground state with increasing solvent polarity and solvent acidity. The highest absolute values of coefficient *s* were found for compounds **1g** and **2d**, and for compounds **1g** and **2b** regarding coefficient *a*. The positive sign of coefficient *b* for most compounds (Tables 3 and 4), except for **1g** and **2i**, indicates a hypsochromic (blue) shift relative to increasing solvent hydrogen-bond accepting capability. This suggests better stabilization of the ground state relative to the excited state. The highest absolute values for coefficient *b* were found for compounds **1e** and **2b**.

Please cite this article in press as: Rančić, M.P. et al., Solvent and substituent effect on intramolecular charge transfer in 5-arylidene-3-substituted-2,4-thiazolidinediones: Experimental and theoretical study. Arabian Journal of Chemistry (2017), http://dx.doi.org/10.1016/j.arabjc.2016.12.013

Table 3 Results of the correlation analysis for series **1** according to Kamlet–Taft equation.

Comp.	h × 10^{-3} (cm^{-1})	s × 10^{-3} (cm^{-1})	b × 10^{-3} (cm^{-1})	a × 10^{-3} (cm^{-1})	R[a]	Sd[b]	F[c]	Solvent excluded from correlation[d]
1a	30.83 ± 0.05	−0.60 ± 0.10	0.09 ± 0.12	−0.14 ± 0.11	0.915	0.11	17	EtOH, MeOH, Dioxane, 2CE, AcN
1b	30.39 ± 0.09	−0.61 ± 0.19	0.34 ± 0.22	−0.58 ± 0.14	0.877	0.19	12	MeOH, 2 ME, Dioxane, AcN
1c	29.38 ± 0.04	−0.08 ± 0.08	0.55 ± 0.11	−0.34 ± 0.07	0.883	0.08	11	1-BuOH, Dioxane, 2CE, 2 ME, iPr_2O
1d	30.33 ± 0.10	−0.60 ± 0.23	0.38 ± 0.30	−0.91 ± 0.24	0.867	0.21	8	MeOH, 1-BuOH, iPr_2O, 2CE, 2 ME, AcN
1e	30.44 ± 0.07	−0.75 ± 0.14	0.64 ± 0.16	−0.57 ± 0.09	0.927	0.14	23	1-PrOH, 2 ME, Dioxane, AcN
1f	30.86 ± 0.06	−0.60 ± 0.12	0.38 ± 0.15	−0.45 ± 0.08	0.928	0.11	23	2 ME, 1,2-DCE, Dioxane, AcN
1g	25.97 ± 0.21	−1.52 ± 0.41	−0.27 ± 0.26	−1.15 ± 0.28	0.932	0.16	24	1-PrOH, 2 ME, 1,2-DCE, AcN
1h	29.37 ± 0.12	−1.23 ± 0.26	0.43 ± 0.32	−0.30 ± 0.11	0.873	0.25	11	1-PrOH, 2 ME, 2CE, Dioxane, AcN
1i	29.94 ± 0.15	−1.23 ± 0.26	0.43 ± 0.32	−0.44 ± 0.24	0.869	0.31	10	MeOH, 1-PrOH, Dioxane, 1,2-DCE, AcN

[a] Correlation coefficient.
[b] Standard deviation.
[c] Fisher test of significance.
[d] Abbreviations for the solvents are given in Table S1.

Table 4 Results of the correlation analysis for series **2** according to Kamlet–Taft equation.

Comp.	h × 10^{-3} (cm^{-1})	s × 10^{-3} (cm^{-1})	b × 10^{-3} (cm^{-1})	a × 10^{-3} (cm^{-1})	R[a]	Sd[b]	F[c]	Solvent excluded from correlation
2a	30.15 ± 0.08	0.83 ± 0.18	0.67 ± 0.18	−0.28 ± 0.14	0.926	0.14	18	Et_2O, Ch, Dioxane, DMF, DMSO, FA
2b	29.63 ± 0.12	0.63 ± 0.29	1.02 ± 0.25	−0.60 ± 0.18	0.871	0.20	10	Dioxane, Ch, 1,2-DCE, DMF, DMSO, FA
2c	29.39 ± 0.07	−11.07 ± 0.14	0.29 ± 0.16	−0.30 ± 0.11	0.925	0.16	26	Dioxane, AcN
2d	30.86 ± 0.16	−1.86 ± 0.20	0.62 ± 0.21	−0.17 ± 0.12	0.953	0.17	30	MeOH, 2 ME, Ch, Hp, Pen, Dioxane
2e	31.21 ± 0.21	−1.75 ± 0.27	0.23 ± 0.24	−0.19 ± 0.16	0.898	0.23	14	MeOH, Ch, Hp, Pen, Dioxane
2f	31.01 ± 0.06	−1.31 ± 0.10	0.66 ± 0.12	−0.14 ± 0.07	0.969	0.30	15	MeOH, 2 ME, Hp, Dioxane
2g	25.18 ± 0.09	−1.67 ± 0.16	0.36 ± 0.18	−0.53 ± 0.12	0.961	0.17	49	Ch, Dioxane, AcN
2h	29.44 ± 0.08	−1.18 ± 0.13	0.25 ± 0.16	−0.15 ± 0.12	0.935	0.15	28	2CE, Dioxane
2i	28.32 ± 0.07	−0.79 ± 0.15	−0.26 ± 0.18	–[d]	0.900	0.53	16	Ch, Hep, Pen, 1,2-DCE

[a] Correlation coefficient.
[b] Standard deviation.
[c] Fisher test of significance.
[d] Negligible values with high standard errors

Results of the quantitative separation of the non-specific solvent effect into polarizability and dipolarity term (coefficients *c* and *d*, respectively), performed by using Catalán equation, are given in Tables 5 and 6.

The results obtained by the use of Catalán equation provide better understanding of attractive/repulsive solvent/solute interactions, and enable an estimation of their appropriate contribution to ν_{max} shift. The correlation results, given in Tables 5 and 6, imply that the solvent polarizability is the principal factor influencing the shift of ν_{max}, whereas solvent dipolarity, acidity and basicity have moderate to low contribution. These results are in accordance with previous study related to 5-arylidene-2,4-thiazolidinediones (Rančić et al., 2012). Negative values of the coefficient *c*, except for compound **1i**, indicate higher contribution of the polarizability effect to the stabilization of the excited state. The noticeable polarizability indicates that the overall π-electronic density shifts take place by two cooperative mechanisms: overall π-network and polarization of localized π-unit (Fig. S1). Interaction of 3-substituted-2,4-thiazolidindione moiety (TZD), which act as an electron-acceptor, with the substituents of different electronic properties causes variation in the mobility of the π-electrons, and thus, a wide range of coefficient *c* values were found. The sensitive balance of both electronic substituent effect and π-electronic interaction in TZD moiety contributes to highest polarizability in compound **1h** (*nitro* substituted derivate) in series **1**, and compound **2i** in series **2**.

A greater extent of resonance interaction is operative within π_1- and π_2-resonance units contributing to higher polarizability of π-conjugated system (Fig. S1). In that context, *dimethylamino* substituent exerts larger π-electron delocalization supported by electron-accepting TZD moiety (similar *c* values were found for both **1g** and **2g**). The phenyl ring present at N3 position in series **2** participates in electron delocalization over TZD which causes electron-density shift to electron-accepting *nitro* substituent present contributing to lower polarizability, *i.e.* coefficient *c* of −2.00 was obtained for **2h** (Table 6).

Effect of solvent dipolarity, assigned with *d* term, is of lower significance and showed complex behavior, with the highest absolute values found for compounds **1d** and **2i**. Dipolar solvent–solute interactions lead to blue shift when a moderate and strong electron-acceptor is present in the arylidene part of the molecule in series **1**. Higher contribution of the solvent

Please cite this article in press as: Rančić, M.P. et al., Solvent and substituent effect on intramolecular charge transfer in 5-arylidene-3-substituted-2,4-thiazolidinediones: Experimental and theoretical study. Arabian Journal of Chemistry (2017), http://dx.doi.org/10.1016/j.arabjc.2016.12.013

Table 5 Results of the correlation analysis for series **1** obtained by using Catalán equation.

Comp.	h	c	d	a	b	R[a]	Sd[b]	F[c]	Solvent excluded from correlation
1a	35.49 ± 0.75	−7.63 ± 1.18	0.89 ± 0.26	−0.88 ± 0.34	−0.32 ± 0.28	0.913	0.21	11	2-PrOH, Ch, DMSO, FA
1b	29.11 ± 0.79	2.06 ± 1.21	−1.07 ± 0.37	−0.71 ± 0.31	0.62 ± 0.32	0.929	0.16	16	MeOH, Dioxane, AcN
1c	33.47 ± 0.84	−6.56 ± 1.29	0.68 ± 0.25	−0.27 ± 0.34	−0.20 ± 0.26	0.903	0.18	9	MeOH, Ch, AcN, DMF, DMSO
1d	34.23 ± 0.64	−6.34 ± 1.01	1.16 ± 0.26	−1.14 ± 0.42	1.17 ± 0.29	0.896	0.20	10	MeOH, Ch, FA
1e	32.01 ± 0.46	−2.43 ± 0.72	0.15 ± 0.19	−1.09 ± 0.23	0.15 ± 0.21	0.904	0.16	12	iBuOH, Dioxane
1f	32.14 ± 0.35	−1.93 ± 0.54	–[d]	−0.84 ± 0.17	−0.13 ± 0.15	0.918	0.12	16	Dioxane
1g	29.34 ± 1.21	−5.28 ± 1.83	−0.32 ± 0.51	−1.90 ± 0.64	−1.18 ± 0.55	0.919	0.44	15	MeOH, 1-PrOH
1h	36.01 ± 0.96	−10.53 ± 1.45	0.80 ± 0.29	0.27 ± 0.46	−0.74 ± 0.32	0.926	0.25	15	EtOH, MeOH, DMSO
1i	28.80 ± 0.91	2.05 ± 1.42	–[d]	−1.34 ± 0.47	−1.12 ± 0.36	0.920	0.27	11	MeOH, 1-PrOH, 2 ME, Dioxane, FA

[a] Correlation coefficient.
[b] Standard deviation.
[c] Fisher test of significance.
[d] Negligible values with high standard errors.

Table 6 Results of the correlation analysis for series **2** obtained by using Catalán equation.

Comp.	h	c	d	a	b	R[a]	Sd[b]	F[c]	Solvent excluded from correlation
2a	31.69 ± 0.37	−2.82 ± 0.58	0.72 ± 0.16	−0.34 ± 0.19	0.87 ± 0.17	0.942	0.14	24	Ch
2b	31.75 ± 0.51	−3.71 ± 0.78	−0.89 ± 0.19	−0.43 ± 0.26	0.88 ± 0.23	0.95	0.18	14	Ch
2c	31.57 ± 0.29	−3.37 ± 0.45	−0.23 ± 0.12	−0.47 ± 0.14	−0.21 ± 0.12	0.972	0.10	53	Dioxane
2d	32.98 ± 0.60	−5.88 ± 0.94	0.38 ± 0.26	−0.18 ± 0.33	1.44 ± 0.27	0.941	0.21	21	Dioxane, 2CE
2e	33.41 ± 0.52	−6.39 ± 0.81	0.59 ± 0.22	−0.48 ± 0.29	1.37 ± 0.24	0.956	0.18	29	Dioxane, 2CE
2f	32.80 ± 0.52	−2.91 ± 0.80	−0.57 ± 0.22	0.34 ± 0.26	0.35 ± 0.23	0.904	0.18	12	Hep, Dioxane
2 g	28.44 ± 0.50	−5.27 ± 0.77	−0.12 ± 0.22	−1.06 ± 0.26	−0.37 ± 0.22	0.960	0.18	35	Ch
2 h	30.59 ± 0.27	−2.00 ± 0.42	−0.99 ± 0.12	0.54 ± 0.14	0.61 ± 0.12	0.976	0.10	57	Hep, Dioxane
2i	33.87 ± 1.14	−6.96 ± 1.31	−2.24 ± 0.46	1.52 ± 0.62	2.30 ± 0.52	0.942	0.40	22	2-PrOH, 2CE

[a] Correlation coefficient.
[b] Standard deviation.
[c] Fisher test of significance.

dipolar effect, in compounds with substituent displaying low/-moderate effect, could be due to balanced contribution of two opposite effects: electronic effect of the substituent and TZD moiety that cause separation of charges by creation of dipolar structure differently oriented in space. The better stabilization of the excited state was found mostly for electron-donor substituted compounds, including **2h**, which indicates that directional shift of electronic density, causes more effective charge separation.

Specific solvent–solute interactions realized through hydrogen bonding, *i.e.* HBD effect can be attributed mainly to the carbonyl groups of the TZD moiety, while solvent basicity (HBA) could be established with generated positive charge at molecular structure. Negative values of the coefficient *a* found in both series **1** and **2**, except **2f**, **2h** and **2i,** indicate moderate to low contribution of the solvent acidity to the stabilization of the excited state. Long-range transmission of substituent effects, which supports the larger polarization of both carbonyl groups, enhances hydrogen bond accepting capabilities of carbonyl oxygens. These observations indicate that solvent achieves the higher extent of hydrogen bonding at nucleophilic sites in TZD moiety.

3.3. LFER analysis of UV–vis data

In an attempt to assess substituent effects on ICT of the investigated compounds, the principles of liner free energy relationships (LFER) were applied to the UV–vis spectral data by using Hammett Eq. (3). The correlation results are given in Tables 7 and 8.

The correlation results (Tables 7 and 8), obtained separately for electron-donating and electron-accepting substituents, reflect different transmission modes of electronic substituent effects through differently oriented π-electronic units (Fig. S1). Obviously, the UV–vis absorption of studied compounds is more substituent–dependent than solvent–dependent (Tables 7 and 8). The introduction of an electron-donor substituent enhances the negative solvatochromism of both series **1** and **2** (Tables 7 and 8, respectively), and also results in a higher susceptibility of the absorption maxima shifts to electronic substituent effects. Somewhat higher sensitivity of ν_{max} to substituent effect was found in solvent with higher proton-donating ability. Significantly lower sensitivity was found for electron-acceptor substituted derivatives in both series **1** and **2**. Such behavior was explained by destabilization

of the TZD moiety by electron-accepting groups (Rančić et al., 2012, 2013), whereas the introduction of either methyl or phenyl group at TZD contributes to low sensitivity to solvent effects. The lowest sensitivities of ν_{max} to substituent effects in nonpolar solvents (pentane and heptane) can be explained by the fact that, at low relative permittivity of surrounding medium, the energy necessary to bring about charge separation in the excited state is relatively high, which gives rise to a lower susceptibility to substituent effects.

3.4. LFER analysis of NMR data

Furthermore, an analysis of the experimental and calculated ^{13}C NMR chemical shifts has been performed to get a better insight into the influence of the substituent effects on *SCS* shifts. The calculated ^{13}C NMR chemical shifts, obtained by the use of GIAO/WP04/aug-cc-pVDZ basis set, are given in Tables S4 and S5. Results of the intercorrelation of experimental and theoretical NMR data are good which indicates that adequate methodology was applied for calculation of theoretical NMR data (Figs. S4–S7). The general conclusion derived from the ^{13}C NMR chemical shifts is that all substituents influence chemical shifts of the carbon atoms of interest (C5, C6, C1′) *via* their electronic effects. LFER principles were applied in the analysis of the substituent effect, defined by σ_p or σ_p^+ substituent constants, on the *SCS* of the carbon atoms of interest. The best correlation results obtained for C5, C6 and C1′ carbons are presented in Table 9.

The observed ρ values for these carbons indicate different susceptibilities of the *SCS* to substituent effects, and it is apparent that chemical shifts of C5 and C1′ showed normal substituent, while reverse substituent effect was observed at C6 for both series **1** and **2**. The negative sign of reaction constant, ρ, for C6 atom means reverse behavior, *i.e.* the value of SCS decreases although the electron-withdrawing ability of the substituents, measured by σ_p, increases. Similar results were obtained in a previous study related to 5-arylidene-2,4-thiazoli dinediones (Rančić et al., 2013) (Tables S6 and S7). The reverse substituent effect operative at C6 can be attributed to localized π-polarization, which predominates over the extended π-polarization (Fig. S8). The π-polarization concept was introduced by Reynolds (Craik and Brownlee, 1983; Reynolds et al., 1983) to explain substituent field effect operative in the side chain of *para*- and *meta*-substituted benzenes. The field effect, induced by substituent dipole, causes secondary polarization of π-electrons in the subsequent independent π-electronic system without net π-electron transfer. According to Reynolds (Craik and Brownlee, 1983; Reynolds et al., 1983), the polar effect mainly arises as a result of the substituent dipole induced field effect, and this effect alters the electron density at C5 by two mechanisms: (i) field-induced polarization of the side chain vinyl group (localized or direct π-polarization) (Fig. S8a), and (ii) field-induced π-electron transfer (extended π-polarization) (Fig. S8b) (Rančić et al., 2013). The second term is the major effect mainly operative in planar systems. Similar influence of substituent from the *meta*- and *para*-positions on C5 supported Reynolds' conclusion that the polar effect is rather of field than of inductive origin (Craik and Brownlee, 1983; Reynolds et al., 1983). The resonance interaction in the extended conjugated system of the substituted styrene molecules in the presence of electron-acceptor substituent has complementary effect to the polarization mechanism (Fig. S8c), and opposite is true for electron-donor substituted compounds.

Table 7 Results of the LFER correlation analysis for series **1** obtained by using Eq. (3).

Comps.	**1a**, **1d**, **1e**, **1f** and **1h**[a]					**1a**, **1b**, **1c**, **1g** and **1i**[b]				
Solvent[c]	$v_0 \times 10^{-3}$ cm^{-1}	$\rho \times 10^{-3}$ cm^{-1}	*R*	*Sd*	*F*	$v_0 \times 10^{-3}$ cm^{-1}	$\rho \times 10^{-3}$ cm^{-1}	*R*	*Sd*	*F*
EtOH	30.99 ± 0.20	−3.07 ± 0.53	0.957	0.33	33	30.96 ± 0.52	8.59 ± 1.31	0.967	0.84	43
MeOH	30.69 ± 0.06	−2.64 ± 0.16	0.994	0.10	269	31.12 ± 0.30	8.31 ± 0.75	0.987	0.48	122
1-PrOH	30.68 ± 0.05	−1.47 ± 0.14	0.986	0.09	107	30.54 ± 0.19	4.68 ± 0.47	0.985	0.30	100
2-PrOH	30.57 ± 0.11	−1.54 ± 0.30	0.948	0.18	27	30.69 ± 0.46	7.38 ± 1.13	0.966	0.73	42
1-BuOH	30.59 ± 0.06	−2.02 ± 0.16	0.990	0.10	152	30.62 ± 0.56	7.41 ± 1.39	0.951	0.89	28
iBuOH	30.57 ± 0.10	−2.08 ± 0.27	0.975	0.17	58	30.86 ± 0.48	7.73 ± 1.18	0.967	0.75	45
2ME	30.94 ± 0.02	−2.24 ± 0.05	0.999	0.03	1950	30.55 ± 0.13	5.16 ± 0.32	0.994	0.21	253
2CE	30.07 ± 0.10	−2.10 ± 0.28	0.973	0.17	55	30.68 ± 0.54	8.46 ± 1.34	0.964	0.85	40
Et_2O	30.82 ± 0.11	−2.09 ± 0.29	0.973	0.18	54	30.93 ± 0.27	6.12 ± 0.67	0.983	0.43	84
iPr_2O	30.98 ± 0.10	−1.95 ± 0.26	0.975	0.16	57	30.94 ± 0.38	7.05 ± 0.94	0.974	0.60	56
Ch	30.91 ± 0.08	−2.35 ± 0.19	0.994	0.10	158	31.17 ± 0.20	6.29 ± 0.49	0.991	0.31	168
Hp	30.92 ± 0.05	−1.97 ± 0.14	0.992	0.09	196	30.98 ± 0.17	5.96 ± 1.68	0.992	0.27	194
Pen	30.95 ± 0.07	−1.99 ± 0.18	0.988	0.11	122	31.01 ± 0.20	5.75 ± 0.49	0.989	0.32	135
1,2-DCE	30.47 ± 0.03	−1.45 ± 0.10	0.995	0.05	323	30.33 ± 0.56	7.11 ± 0.69	0.986	0.44	107
Dioxane	30.06 ± 0.13	−2.67 ± 0.34	0.976	0.21	61	29.84 ± 0.28	7.00 ± 0.70	0.985	0.45	100
AcN	31.05 ± 0.09	−1.58 ± 0.22	0.970	0.14	48	31.33 ± 0.34	7.29 ± 0.84	0.981	0. 54	76
DMSO	30.49 ± 0.19	−2.57 ± 0.51	0.949	0.32	27	30.97 ± 0.46	7.63 ± 1.14	0.968	0.73	45
DMF	30.66 ± 0.16	−2.73 ± 0.53	0.965	0.27	40	31.07 ± 0.47	8.40 ± 1.16	0.972	0.74	52
FA	30.35 ± 0.21	−2.80 ± 0.56	0.944	0.35	25	30.96 ± 0.41	8.72 ± 1.01	0.980	0.65	74

[a] Electron-acceptor substituted compounds.
[b] Electron-donor substituted compounds.
[c] Abbreviations for the solvents are given in Table S1.

Please cite this article in press as: Rančić, M.P. et al., Solvent and substituent effect on intramolecular charge transfer in 5-arylidene-3-substituted-2,4-thiazolidinediones: Experimental and theoretical study. Arabian Journal of Chemistry (2017), http://dx.doi.org/10.1016/j.arabjc.2016.12.013

Table 8 Results of the LFER correlation analysis for series **2** obtained by using Eq. (3).

Comps.	**2a**, **2d**, **2e**, **2f** and **2h**[a]					**2a**, **2b**, **c**, **2g** and **2i**[b]				
Solvent	$v_0 \times 10^{-3}$ cm^{-1}	$\rho \times 10^{-3}$ cm^{-1}	*R*	*Sd*	*F*	$v_0 \times 10^{-3}$ cm^{-1}	$\rho \times 10^{-3}$ cm^{-1}	*R*	*Sd*	*F*
EtOH	30.89 ± 0.05	−2.25 ± 0.13	0.995	0.08	289	31.13 ± 0.21	8.52 ± 0.53	0.994	0.34	258
MeOH	30.03 ± 0.05	−2.28 ± 0.13	0.995	0.08	308	30.47 ± 1.11	7.39 ± 2.47	0.904	1.37	10
1-PrOH	30.03 ± 0.03	−2.38 ± 0.08	0.992	0.05	785	31.23 ± 0.46	8.200.46	0.995	0.29	316
2-PrOH	30.99 ± 0.05	−2.12 ± 0.13	0.994	0.08	251	30.86 ± 0.48	7.85 ± 1.20	0.967	0.77	43
1-BuOH	30.95 ± 0.04	−2.28 ± 0.12	0.996	0.07	393	31.14 ± 0.17	8.15 ± 0.42	0.996	0.27	373
iBuOH	30.89 ± 0.03	−2.12 ± 0.09	0.997	0.05	620	31.15 ± 0.22	8.20 ± 0.54	0.993	0.35	227
2 ME	30.34 ± 0.06	−2.74 ± 0.17	0.994	0.14	262	31.10 ± 0.22	8.48 ± 0.54	0.994	0.34	246
2CE	30.61 ± 0.07	−2.42 ± 0.17	0.992	0.11	198	30.78 ± 0.20	8.32 ± 0.49	0.995	0.32	283
Et_2O	31.08 ± 0.08	−2.21 ± 0.16	0.992	0.10	194	31.35 ± 0.24	7.50 ± 0.58	0.991	0.37	165
iPr_2O	30.98 ± 0.10	−1.95 ± 0.26	0.975	0.16	57	31.24 ± 0.23	7.38 ± 0.58	0.991	0.37	161
Ch	31.03 ± 0.03	−2.26 ± 0.07	0.999	0.04	1036	31.34 ± 0.29	8.38 ± 0.71	0.989	0.46	139
Hp	29.96 ± 0.02	−0.58 ± 0.05	0.997	0.03	143	30.41 ± 0.32	6.18 ± 0.79	0.977	0.50	62
Pen	29.99 ± 0.03	−0.71 ± 0.09	0.975	0.06	59	30.47 ± 0.29	6.08 ± 0.72	0.980	0.46	71
1,2-DCE	30.68 ± 0.04	−2.12 ± 0.10	0.997	0.06	484	30.76 ± 0.31	7.20 ± 0.77	0.983	0.49	87
Dioxane	30.02 ± 0.06	−2.39 ± 0.16	0.993	0.10	227	30.33 ± 0.17	7.30 ± 0.42	0.995	0.27	302
AcN	30.67 ± 0.06	−2.82 ± 0.16	0.971	0.25	49	30.40 ± 0.67	6.54 ± 1.68	0.914	1.07	15
DMSO	30.53 ± 0.17	−2.57 ± 0.45	0.957	0.27	33	30.46 ± 0.71	7.88 ± 1.76	0.932	1.13	20
DMF	30.29 ± 0.19	−2.67 ± 0.51	0.950	0.31	28	30.24 ± 0.72	7.98 ± 1.79	0.932	1.14	20
FA	29.86 ± 0.22	−2.01 ± 0.57	0.897	0.35	12	29.99 ± 0.63	8.12 ± 1.56	0.949	1.00	27

[a] Electron-acceptor substituted compounds.
[b] Electron-donor substituted compounds.

It can be noticed, from Table 9, that correlations with electrophilic substituent constants, σ_p^+, are of better quality for C6 and C1′ atoms in series **1**, and C5 and C1′ atoms in series **2**. It indicates higher contribution of extended resonance interaction for these carbons. Introduction of the *methyl* or *phenyl* group in series **1** and **2**, respectively, decreases susceptibility of the C5 and C1′ atoms to substituent effects in comparison with previous result (lower ρ) (Rančić et al., 2013), while increased susceptibility of the C6, for both series **1** (−7.03), and series **2** (−3.32; Table 9), was found. Sensitivity of *SCS* to substituent effects is mainly determined by three factors: conformational arrangement, substituent effects and introduction of *methyl* or *phenyl* group at N3-position of TZD which contributes to specific shift of electronic density at the carbon atom of interest.

To evaluate separate contributions of the polar (inductive/-field) and resonance effects, the regression analysis according to DSP Eq. (4), *i.e.* Reynold's equation, with σ_F and σ_R^o substituent constants has been performed and the results are given in Table 10.

The success of the fitting is not improved by using DSP equation, but it helps in better understanding of the transmission mode of substituent effect. The positive ρ_F and ρ_R values were obtained for the C5 and C1′ atoms, while negative values are obtained for C6 carbon. The positive values of ρ_F and ρ_R for the C5 atom and negative values for the C6 atom show that substituents in a different way influence the π electron density at carbon atoms in a side chain. The negative ρ_F value for the C6 atom of both series is an indication of the opposite substituent effect, the so-called reverse substituent effect (RSE),

Table 9 Result of correlations of the *SCS* values of C5*, C6* and C1′ carbons *versus* σ_p/σ_p^+ substituent constants for series **1** and **2,** obtained by using SSP equation.

	Atom		ρ	*h*	*R*	*F*	*sd*
Series **1**	C5	σ_p	9.94 ± 0.73	0	0.984	187	0.89
		σ_p^+	6.04 ± 0.76	1.40 ± 0.56	0.955	63	1.50
	C6	σ_p	−7.03 ± 1.41	−1.14 ± 0.48	0.912	25	1.20
		σ_p^+	−4.40 ± 1.53	−2.07 ± 0.68	0.790	8	1.79
	C1′	σ_p	12.15 ± 1.39	−2.36 ± 0.60	0.963	77	1.71
		σ_p^+	7.80 ± 0.51	−0.55 ± 0.37	0.988	236	1.00
Series **2**	C5	σ_p	6.63 ± 0.63	−0.96 ± 0.28	0.974	109	0.78
		σ_p^+	4.25 ± 0.17	0.02 ± 0.12	0.995	658	0.32
	C6	σ_p	−3.32 ± 0.49	−0.62 ± 0.21	0.940	46	0.60
		σ_p^+	−1.94 ± 0.43	−1.07 ± 0.31	0.879	20	0.84
	C1′	σ_p	12.35 ± 1.72	1.99 ± 0.75	0.946	51	2.12
		σ_p^+	7.84 ± 0.94	−0.17 ± 0.69	0.959	69	1.85

* C5 and C6 are equivalent to C_β and C_α, respectively, used in a previous study (Rančić et al., 2012).

Please cite this article in press as: Rančić, M.P. et al., Solvent and substituent effect on intramolecular charge transfer in 5-arylidene-3-substituted-2,4-thiazolidinediones: Experimental and theoretical study. Arabian Journal of Chemistry (2017), http://dx.doi.org/10.1016/j.arabjc.2016.12.013

which is due to π-polarization. The π-polarization concept can also explain the larger magnitude of polar effects at C6 in series **1** (ρ_F = –8.69), which is related to the strength of the resonance interaction between the *para*-carbon (C1′) and *para*-substituent present. All λ values are higher than 1, except for C6 atoms in series **1** and **2**, which means that resonance effect predominates over field effect, and highest effect was found for C1′ carbon. The extent of resonance interaction depends on spatial arrangement of the molecules, *i.e.* the values of torsional angle θ, and thus, the resonance substituent effect is most effectively transmitted to C1′ carbon.

Value of the term ρ_R, *i.e.* the effect of π-electron delocalization, and the term ρ_F, attributed to the effect of substituent induced π-polarization, significantly depends on the electronic system present at C5 carbon. The ρ_F value for C5 and C6 atoms reflects mainly field effect, which is the most pronounced in series **1** when *methyl* group is present at N3 atom. Introduction of phenyl ring at N3-position compensates for electron-accepting power of TZD by increasing π-electron density, and causing lower extent of extended π-electron delocalization (ρ_R = −2.92 and −5.20 for series **2** and **1**, respectively; Table 10).

The electron-accepting carbonyl group present in TZD moiety tends to decrease electron density at the vinyl side chain resulting in strong resonance interaction with *para*-electron–donating substituents. Electron-donors cause the increase of electron density in the arylidene ring which, therefore, acts as π-donor and causes increase in resonance interaction with the vinyl side chain. Synergism of these effects causes pronounced electron density changes at the C5 atom. Oppositely, in the case of electron-accepting substituent, balanced and oppositely directed interactions of two electron-accepting moieties determine such behavior where both parts exert appropriate response to electronic demand of the rest of molecule, and the consequence is the higher extent of localized π-polarization at C5 atom. The net result is that the electron-accepting substituents increase the electron density on the C6 atom due to π-polarization.

3.5. Comparative LFER analysis of SCS for C5 and C6 in styrene series 1–10

The study of the mechanism of transmission of electronic substituent effects in an aromatic framework with a side chain, *i.e.* β-substituted styrene derivatives (Fig. S9) is very useful in order to distinguish the contribution of polar (field/inductive) and polarization effects (Craik and Brownlee, 1983) at carbon of interest. The substituent dipole polarizes the vinyl π-electron resulting in separation of opposite charges at neighboring atoms which depends on heterocyclic system attached at C5 carbon. In order to get deeper insights into factors determining such phenomena, a comprehensive analysis of the electronic and structural effect was performed for series **1** and **2** and compared with results obtained for eight styrene series **3**–**10** (Fig. S9) (Rančić et al., 2013; Reynolds et al., 1983; Hamer et al., 1973a, 1973b; Tan et al., 1987; Krabbenhoft, 1978; Cornelis et al., 1981). Saleh et al. (2008) have studied 19 styrene series and concluded that different groups (Fig. S9) of the side chain have significant effects on *SCS* of C5 carbon. Due to this selection of a wide range of structurally different groups present at C5 atom in series **1**–**10** offered a good base of data used in a systematic LFER analysis.

Results of LFER analysis for the C5 and C6 atoms of series **3**–**10**, in the form of SSP equation with σ_p or σ_p^+ constants, are presented in Tables S8 and S9, respectively (Rančić et al., 2013). Normal and reverse substituent effects were observed at C5 and C6 atoms, respectively, for all studied compounds. Two groups of correlation results could be recognized for the C5 atom: series **3**–**6**, including series **1** (9.94; Table 10), and series **7**–**10**, including series **2** (6.63; Table 10). Values of the coefficient ρ for C6 are similar for series **2**–**10** with the highest value of −3.34 found for series **9** (Table S9). Exceptionally higher ρ values of −7.03 for series **1** were found (Table 9). The correlation results for the C5 atom are significantly improved when electrophilic substituent constant σ_p^+ is used in correlation for series **1** and **4**–**9**, while this does not apply for the series **2**, **3** and **10**. The terminal C5 atom in vinyl group suffers from electron deficiency, and thus *SCS* in series **1** and **4**–**9** better correlates with σ_p^+. The correlation results are of lower quality for the correlation for C6 *SCS* with σ_p^+ indicating lower contribution of the extended resonance interaction.

Previous results of LFER analysis for series **3**–**10**, obtained by using DSP model are given in Tables S10 and S11 (Rančić et al., 2013). The magnitude of resonance coefficient, ρ_R, for C5 is twice (series **5**) or more than twice larger (series **3** and **7**–**9**) than the field effect emphasizing the significance of resonance interaction at C5 atom. It is worth of noting a significantly lower contribution of ρ_R, *i.e.* lower λ values for C6 of series **4**–**8** and **10**. The number of systematic studies also revealed higher sensitivity of *SCS* at C5 due to the greater contribution of resonance effects (Craik and Brownlee, 1983; Reynolds et al., 1983; Hamer et al., 1973a, 1973b; Tan et al., 1987; Krabbenhoft, 1978; Cornelis et al., 1981; Saleh et al., 2008). The Reynolds ρ_F values for the C5 atom reflect the pure field effect which is most pronounced in series **3.** Delocalization of the lone electron pair in amide group (structure I; Fig. S10) contributes to an excess of electron density and,

Table 10 Correlation results of the *SCS* values for C5, C6 and C1′ carbons for series **1** and **2** with the DSP equation.

	Atom	ρ_F	ρ_R	*R*	*F*	*sd*	$\lambda = \rho_R/\rho_F$
Series **1**	C5	9.67 ± 1.64	10.89 ± 1.09	0.984	79	0.97	1.13
	C6	−8.69 ± 1.94	−5.20 ± 2.05	0.936	14	1.15	0.60
	C1′	7.56 ± 2.08	14.57 ± 1.39	0.984	76	0.97	1.93
Series **2**	C5	4.49 ± 0.93	7.76 ± 0.62	0.989	113	0.55	1.72
	C6	−4.06 ± 1.03	−2.92 ± 0.69	0.948	22	0.62	0.72
	C1′	7.67 ± 3.07	14.82 ± 2.06	0.967	36	1.83	1.93

Please cite this article in press as: Rančić, M.P. et al., Solvent and substituent effect on intramolecular charge transfer in 5-arylidene-3-substituted-2,4-thiazolidinediones: Experimental and theoretical study. Arabian Journal of Chemistry (2017), http://dx.doi.org/10.1016/j.arabjc.2016.12.013

hence, the sensitivity of the C5 atom to the field effect is increased. Competitive resonance interaction (structures I and II; Fig. S10) participates in a different extent in *SCS* change at C5 and C6 depending on substituent present. Electron-donors support increased contribution of structure II (Fig. S10), oppositely, electron-acceptors suppress to some extent extended π-delocalization favoring amide resonance (structure I; Fig. S10). Introduction of *methyl* group, present in series **1**, exerts negligible effect by supporting amide group resonance. In the other hand, the presence of phenyl ring in series **2** contributes to aniline type *n*,π-resonance interaction supporting resonance presented by structure II (Fig. S10).

The structural similarity of series **3** and **9** offers a possibility to compare correlation results in relation to structural difference of heterocyclic structure attached at C5 atom. The correlation results for the C5 and C6 atoms (Tables S10 and S11, respectively) indicate that, not only electronic properties of heteroatoms, but also geometrical characteristics, *i.e.* planar hydantoines (Tan et al., 1990), and non-planar 5-arylidene-2,4-thiazolidindiones (Table S12) influence their specific behavior. Moreover, similar λ values for the C5 (2.09 and 2.82) and C6 (1.46 and 1.14) atom for series **3** and **9**, respectively, were found, while larger differences were observed with respect to other series. In hydantoines there is a competitive contribution of two resonance structures (Fig. S11) depending on substituent present. According to correlation results, N1 lone pair delocalization contributes to lower ρ_R at C5 (7.52 *versus* 17.03 for series **9** and **3**, respectively; Table S10). Anyway, resonance interaction at C5 is of high contribution (λ = 2.82; Table S10), indicating significant π,π-delocalization within heterocyclic moieties. Comparing the series **6**–**8** to series **4** and **5**, it can be noted that strong electron-accepting substituents, *chloro* and *cyano* group, enhance sensitivity of C5 carbon to resonance effect (Table S10), while two carbonyl groups adjacent to the C5 atom in series **6**–**8** exert appreciable extent of electron-accepting properties. Correlation results for series **6**–**8** show a decrease in field and resonance effect for C5 (Table S10), while the λ values are high with decreasing order from series **4** to series **6**. This order indeed reflects ability of electronic density at the C5 carbon to interact with two neighboring carbonyl groups which in turn might competitively resonate with lone electron pair at oxygen (series **4**) or nitrogen (series **5**) and phenyl π-electrons (series **6**).

A more complex situation was found for C6 because this carbon senses the electronic effect of the substituted phenyl ring and heterocyclic moiety; hence, no regularity of correlation results was found for this carbon. There are some similarity regarding ρ_F values (Table S11), with the highest ones found for series **1**, **2**, **7** and **8.** However, low λ values, obtained for all series (λ < 1, except for series **3** and **9**), indicate a lower contribution of resonance effect which is likely due to balanced/opposed effect of the substituent and heterocyclic moiety resulting in the higher contribution of the π-polarization at this carbon.

Generally, it might be concluded that, according to results of LFER studies (Tables 9 and 10 and S8–S11), transmission of substituent electronic effects through defined π-resonance units indicates that these units, behave either as isolated or as conjugated fragments depending on substituents present in the corresponding molecule. The significance of extended π, π-delocalization through defined π-resonance units of series **1** (Scheme 1) is mainly operative within π-resonance units with high contribution of π-polarization at C5 carbon. The opposite is true for C6 atom for series **2**–**8** and **10** where significant π,π-delocalization is observed within heterocyclic moieties. Also, Brownlee et al. (Craik et al., 1982) concluded that the differences in geometry affect the ratios of the ρ_R values for different styrene series, and not the ratio of the ρ_R values for the C5 and C6 carbons in the same series.

3.6. MP2 and TD-DFT calculations. Evaluation of electronic transition and ICT

Theoretical calculations can complement experimental investigations, *i.e.* to validate experimental conclusions, or even upgrade with some confidence into experimental unexplored area. In that context, as first step, it was necessary to perform optimization of the geometries of the investigated molecules by the use of *ab initio* MP2 method. The significant stability of the *Z* isomer was obtained, and energies related optimized geometries are presented in Table S13, and optimized structures of series **1** and **2**, in acetonitrile, are given in Figs. S11 and S12, respectively. Similar results were obtained for gas phase. Elements of the optimized geometries of investigated compounds, (*Z*)-5-arylidene-3-methyl-2,4-thiazolidinediones (series **1**) and (*Z*)-5-arylidene-3-phenyl-2,4-thiazolidinediones (series **2**), obtained by the use of MP2/6-31G(d,p) method, are given in Tables S14 and S15.

It can be seen that geometric features of the studied TZDs of both series follow the similar trend related to geometry parameter change *versus* substituent effect. Consideration of the torsional angles θ (Fig. S1), defined by out-of-plane rotation of the phenyl ring with respect to the exocyclic double bond, and their changes (Tables S14 and S15) indicates that introduction of substituent induces decreasing the θ values. Similar trend was found for 5-arylidene-2,4-thiazolidinediones (Table S8) (Rančić et al., 2013). The introduction of electron-donor substituent causes increase of N3—C4 and both carbonyl groups' bond lengths, while, oppositely, decrease of C4—C5, N3—CH_3, as well as N3—Ph, C6—C1′ and C2—N3 bond lengths was found. The most pronounced effect was found for *dimethylamino* group which supports an electron density shift from the π_1-unit to the electron-accepting TZD moiety contributing to higher planarization of molecule and greater extent of the π,π-delocalization. This result is an additional support for the extended conjugation operative in the π_1- and π_2-unit, *i.e.*, the π-electron density shifts toward C4═O carbonyl group causing increase in both carbonyl groups bond lengths.

The opposite is true for electron-acceptor substituted compounds. Higher electron-acceptor ability of the substituent causes increase in θ values and C4—C5 bond length which indicates that contribution of two opposite effects: electron-accepting arylidene group and TZD carbonyl groups cause geometry adjustment together with low sulfur positive resonance participation as a response to electronic demand of the electron deficient environment. The normal carbonyl groups' polarization is suppressed and causes a slight bond length decrease.

Furthermore, it was shown that interpretation of the UV–Vis spectra was achieved by the use of TD-DFT quantum chemical calculations given on 1-(1-naphthoyl)-3-(halo-phenyl)-thioureas (Saeed et al., 2015). Mechanism of electronic

Please cite this article in press as: Rančić, M.P. et al., Solvent and substituent effect on intramolecular charge transfer in 5-arylidene-3-substituted-2,4-thiazolidinediones: Experimental and theoretical study. Arabian Journal of Chemistry (2017), http://dx.doi.org/10.1016/j.arabjc.2016.12.013

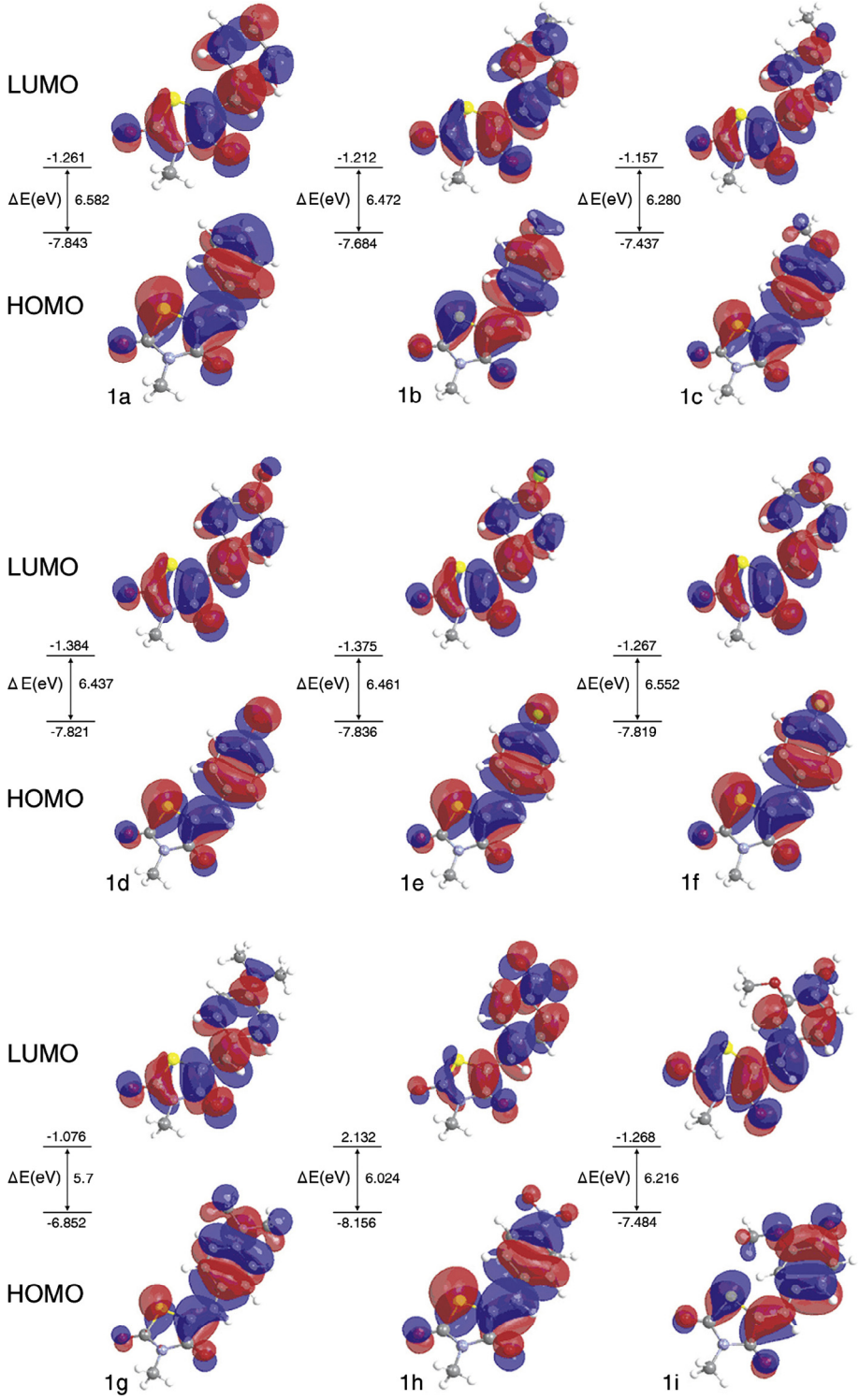

Figure 2 The HOMO/LUMO orbitals and E_{gap} of compounds **1a**–**1i** in acetonitrile.

excitations and changes in the overall charge distribution in both ground and excited states of the investigated molecules were studied by calculation of HOMO/LUMO energies (E_{HOMO}/E_{LUMO}) and E_{gap} values in solvent acetonitrile. Obtained results are presented in Figs. 2 and 3, and Table S16. Generally, E_{gap} values were lower than for unsubstituted compound in both series, and also lower values were obtained for series **2** with the lowest ones found for compounds **1g** and **2g**. No significant ICT could be noticed from the structure of frontier orbitals, but it could be observed similarity of orbital independently on the presence of *methyl* or *phenyl* group in N3-position of studied compounds. Unsubstituted compounds have the largest energy gaps of 6.582 eV (**1a**) and 6.542 eV (**2a**), while the lowest energy gaps were observed

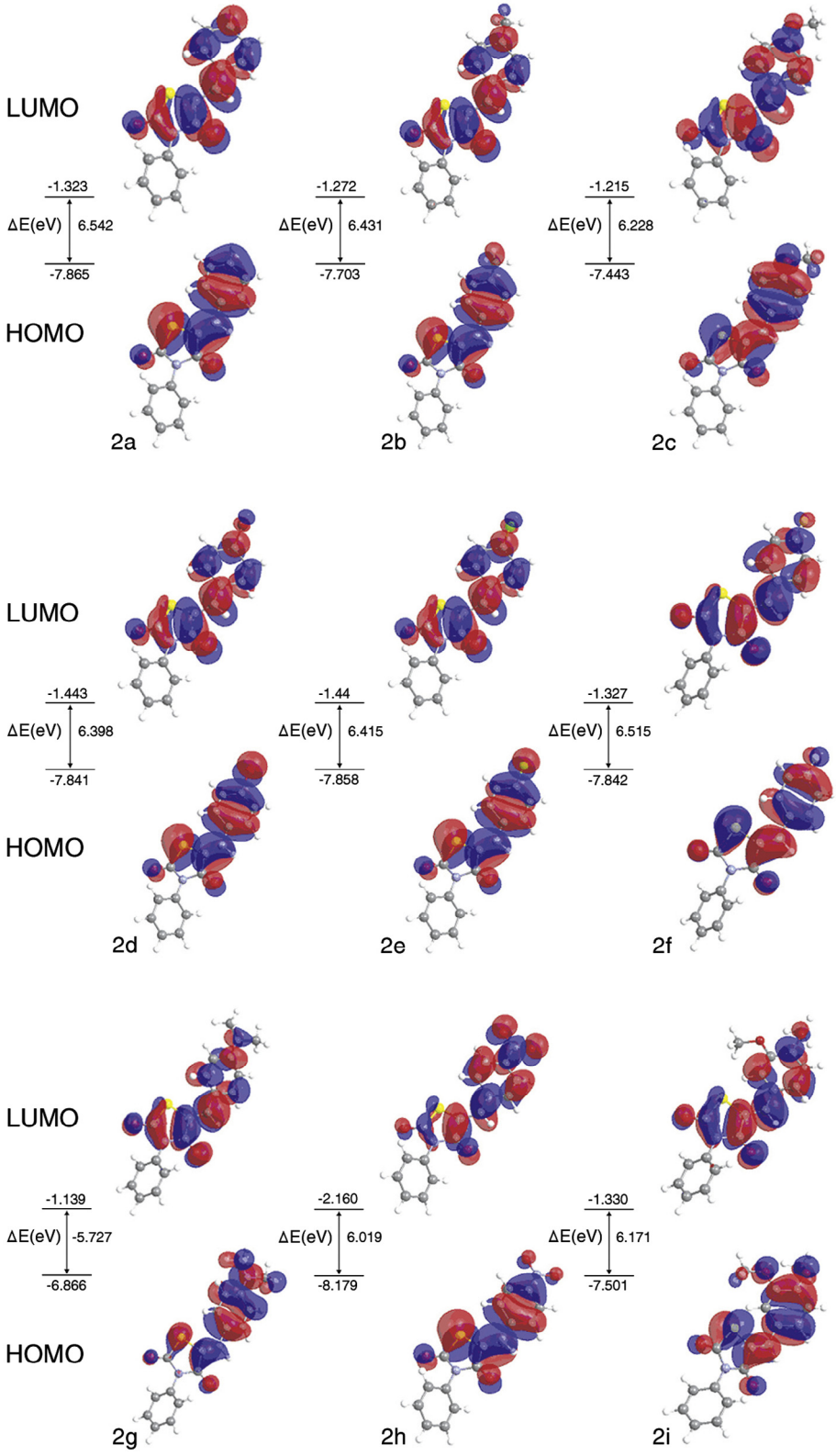

Figure 3 The HOMO/LUMO orbitals and E_{gap} of compounds **2a**–**2i** in acetonitrile.

for compounds **1g** and **2g** with 5.776 and 5.727 eV, respectively. This is consistent with the largest bathochromic shift of their absorption maxima. Obviously, the ICT process is more feasible in more planar compounds **1g** and **2g** due to higher polarizability of excited state which can be, under influences of surrounding solvent environment, preferentially stabilized with respect to the ground state (Table 11). Due to this, the excited and ground states are closer and more rapid inter-

Please cite this article in press as: Rančić, M.P. et al., Solvent and substituent effect on intramolecular charge transfer in 5-arylidene-3-substituted-2,4-thiazolidinediones: Experimental and theoretical study. Arabian Journal of Chemistry (2017), http://dx.doi.org/10.1016/j.arabjc.2016.12.013

nal conversion is permitted. Variation of substituent patterns clearly indicates that contributions of both structural and substituent/compound donor-acceptor character are involved in the ICT mechanism of the investigated molecules. Additional results of TD-DFT calculations, oscillator strengths, vertical excitation energies and electronic transitions are provided in Table 11, since the TD-DFT results have indicated a large contribution of single HOMO to LUMO excitations in ground to first excited state transition (greater than 90% for all compounds; Table 11). Only in the case of *nitro* substituted compounds (**1h** and **2h**), there is small participation of HOMO to LUMO + 1 excitation (< 5%). In conclusion, all compounds showed bathochromic shift compared to unsubstituted compounds in solvent acetonitrile for both series, and the lowest E_{gap} values were observed for compounds **1g** and **2g** form. These results are consistent with experimental ones.

ICT occurs when photon absorption promotes a significant deformation of the electronic cloud due to appropriate (partial/total) electronic shift from one moiety of a molecule to another. In order to quantify this phenomenon, a simple and efficient model was used for definition/evaluation of ICT on the basis of the overall charge distribution computed and changes in the both ground and excited states (Le Bahers et al., 2011; Jacquemin et al., 2012; Ciofini et al., 2012). TD-DFT method was used for quantification of the ICT by calculations of the charge-transfer distance (D_{CT}), amount of transferred charge (Q_{CT}), and the value of variation of dipole moment between the ground and excited states (μ_{CT}). Excitation of a molecule by a photon may cause a transfer of charges from one part to another part of a molecule leading to conformational changes in the excited state, which result in a change of dipole moment in the excited state compared to ground state.

Practically, the knowledge of the excited state dipole moment is quite useful in designing nonlinear materials or allows one to estimate the site of electrophilic or nucleophilic attacks in some photochemical reactions. Results of calculated distance between two barycenters of the density depletion and

Table 11 Results of TD-DFT calculations for transitions from ground to first vertical excited state for series **1** and **2** in solvent acetonitrile.

Comp.	Energy (eV)	Oscillator strength	Excitation	CI expansion coefficient	% of single particle excitation contribution
1a	4.0390	0.6700	HOMO → LUMO	0.69869	97.6
1b	3.9671	0.7674	HOMO → LUMO	0.69741	97.3
1c	3.8494	0.8002	HOMO → LUMO	0.69312	96.1
1d	3.9513	0.8192	HOMO → LUMO	0.69376	96.3
1e	3.9647	0.7854	HOMO → LUMO	0.69620	96.9
1f	4.0288	0.6771	HOMO → LUMO	0.69764	97.3
1g	3.5452	0.9968	HOMO → LUMO	0.68546	94.0
			HOMO − 1 → LUMO	0.12094	2.90
1h	3.7204	0.7741	HOMO → LUMO	0.67632	91.5
			HOMO → LUMO + 1	−0.15096	4.60
1i	3.8294	0.7659	HOMO → LUMO	0.68843	94.8
2a	4.0029	0.7661	HOMO → LUMO	0.69803	97.4
2b	3.9305	0.8799	HOMO → LUMO	0.69671	97.1
2c	3.8158	0.9778	HOMO → LUMO	0.69285	96.0
2d	3.9167	0.9275	HOMO → LUMO	0.69307	96.1
2e	3.9317	0.8909	HOMO → LUMO	0.69557	96.8
2f	3.9951	0.7835	HOMO → LUMO	0.69684	97.1
2g	3.5007	1.1189	HOMO → LUMO	0.68483	93.8
2h	3.7054	0.8683	HOMO → LUMO	0.67630	91.5
			HOMO → LUMO + 1	−0.14792	4.40
2i	3.7897	0.8679	HOMO → LUMO	0.68771	94.6

Table 12 Calculated values of D_{CT}, Q_{CT}, and μ_{CT} during electron excitation.

Molecule	Q_{CT} (e^-)	D_{CT} (Å)	μ_{CT} (D)	Molecule	Q_{CT} (e^-)	D_{CT} (Å)	μ_{CT} (D)
1a	0.501	1.389	0.696	**2a**	0.500	1.416	0.708
1b	0.506	1.558	0.788	**2b**	0.506	1.631	0.825
1c	0.528	2.101	1.109	**2c**	0.531	2.139	1.136
1d	0.501	1.548	0.776	**2d**	0.499	1.592	0.794
1e	0.499	1.467	0.589	**2e**	0.497	1.508	0.749
1f	0.509	1.478	0.752	**2f**	0.507	1.531	0.776
1g	0.567	2.939	1.666	**2g**	0.566	2.980	1.687
1h	0.737	0.989	0.729	**2h**	0.736	0.988	0.727
1i	0.554	2.255	1.249	**2i**	0.553	2.307	1.276

Please cite this article in press as: Rančić, M.P. et al., Solvent and substituent effect on intramolecular charge transfer in 5-arylidene-3-substituted-2,4-thiazolidinediones: Experimental and theoretical study. Arabian Journal of Chemistry (2017), http://dx.doi.org/10.1016/j.arabjc.2016.12.013

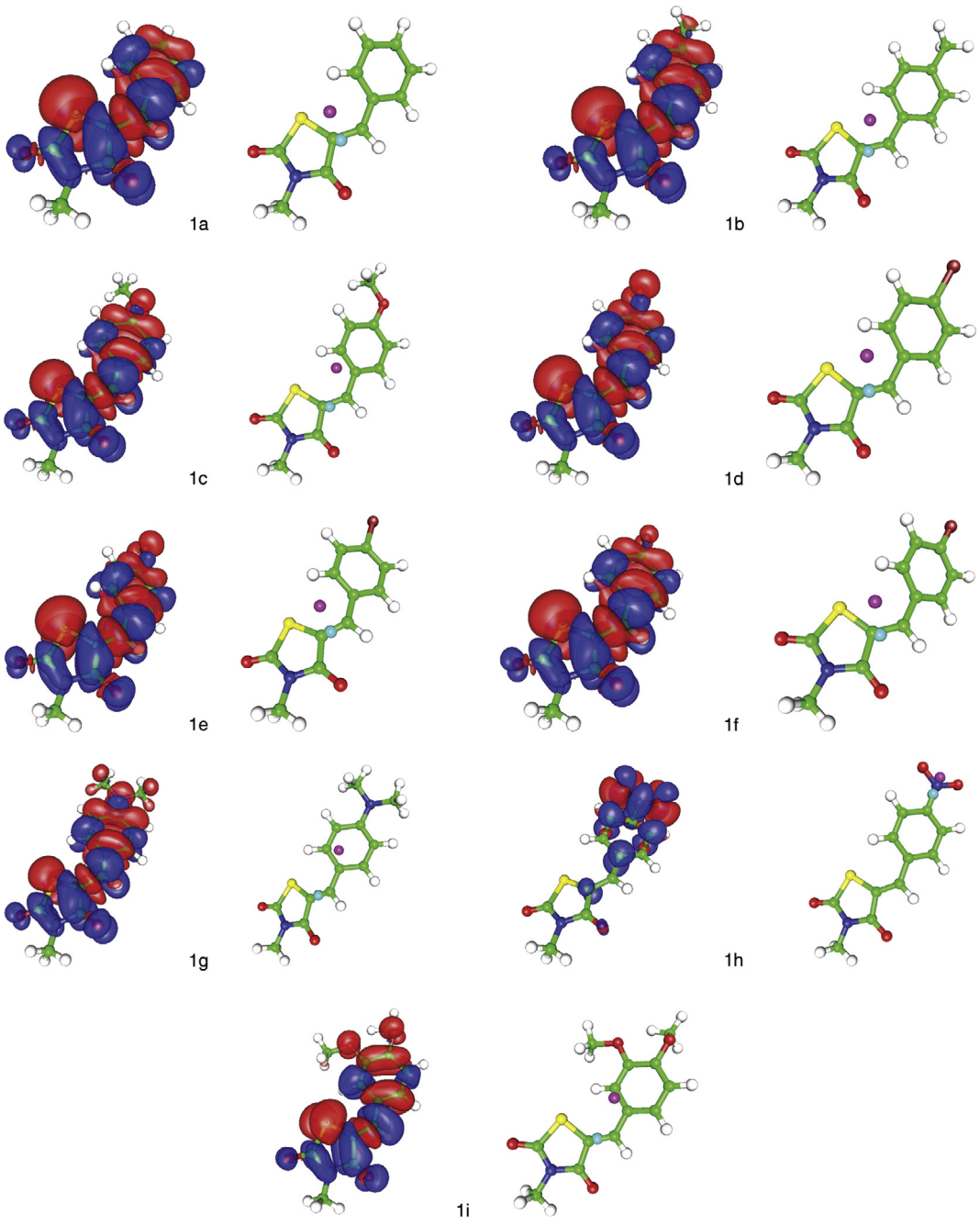

Figure 4 ICT processes in compounds **1a–1i**; Left images – difference between densities in excited and ground state (red and blue – density increase and decrease upon transition, respectively); Right images – positions of barycenters describing charge loss (cyan circle) and charge gain (violet circle) upon transition.

the density increment zones (D_{CT}), Q_{CT} and μ_{CT} change during electron excitation are presented in Table 12. In general most of ICT take place by electron density shift from TZD to arylidene part of molecule during electronic transition. It is noticeable that the strongest ICT occurs in **1g** and **2g**, *i.e. dimethylamino* substituted compound, showing transfer of 0.567 e^- over 2.939 Å and 0.566 e^- over 2.980 Å, respectively. On the other hand, in molecules **1h** and **2h** *nitro* substituted derivatives, intramolecular charge transfer of 0.737 e^- over 0.989 Å and 0.736 e^- over 0.988 Å, respectively, is an evidently local process which occurs within *nitro* substituent (Figs. 4 and 5).

The variation of substituent patterns indicates that contributions of both conformational arrangement and donor–accepting character are involved in the ICT mechanism of the investigated molecules (Figs. 4 and 5).

MEP (molecular electrostatic potential) analysis was used to evaluate and visualize charge distribution over investigated compounds, and illustrate the three dimensional charge distributions overall investigated molecules. MEP potential at a point in space around a molecule gives information about the net electrostatic effect produced at that point by total charge distribution (electron + proton) of the molecule and

Please cite this article in press as: Rančić, M.P. et al., Solvent and substituent effect on intramolecular charge transfer in 5-arylidene-3-substituted-2,4-thiazolidinediones: Experimental and theoretical study. Arabian Journal of Chemistry (2017), http://dx.doi.org/10.1016/j.arabjc.2016.12.013

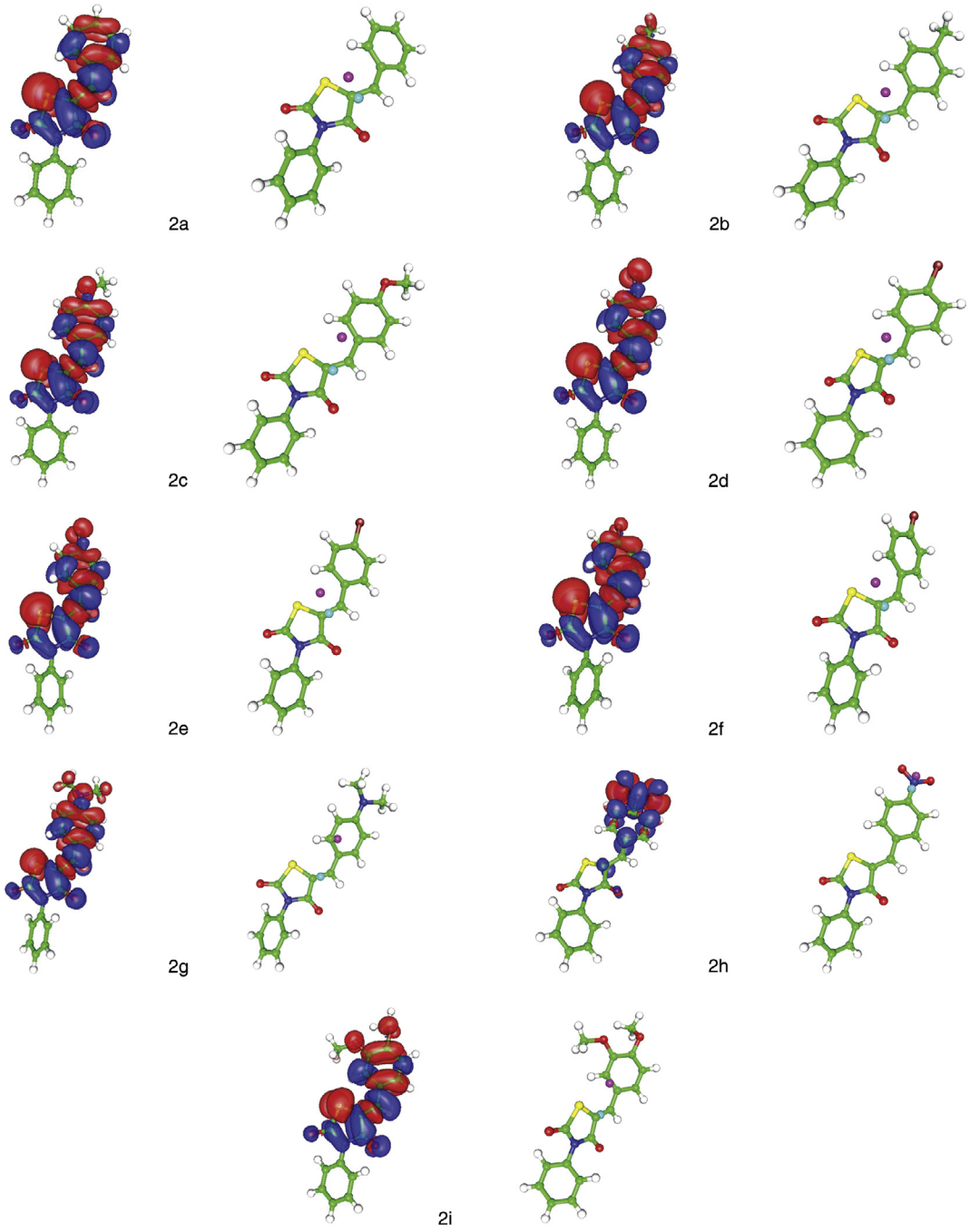

Figure 5 ICT processes in compounds **2a–2i**; Left images – difference between densities in excited and ground state (red and blue – density increase and decrease upon transition, respectively); Right images – positions of barycenters describing charge loss (cyan circle) and charge gain (violet circle) upon transition.

correlates with dipole moments, electro-negativity, partial charges and chemical reactivity of the molecules. It provides a visual method to understand the relative polarity of the molecule (Reynolds et al., 1983). An electron density isosurface mapped with electrostatic potential surface depicts the size, shape, charge density and site of chemical reactivity of the molecules. MEP shown in Figs. S13 and S14 illustrates the three dimensional charge distributions overall investigated molecules. The values of the electrostatic potential at the surface are represented by different colors; red represents regions of most electronegative electrostatic potential, it indicates the region of high electron density, *i.e.* sites favorable for electrophilic attack (favorable site for HBD solvent to solute interactions); blue represents regions of the most positive electrostatic potential, *i.e.* region of low electron density favorable for nucleophilic attack (preferential solvent/solute HBA interactions), and green represents regions of zero potential. Potential increases in the order red < orange < yellow <

Please cite this article in press as: Rančić, M.P. et al., Solvent and substituent effect on intramolecular charge transfer in 5-arylidene-3-substituted-2,4-thiazolidinediones: Experimental and theoretical study. Arabian Journal of Chemistry (2017), http://dx.doi.org/10.1016/j.arabjc.2016.12.013

green < blue. The blue color indicates the strong attractive potential, region favorable for HBA solvent interactions, while red color indicates the repulsive potential, and includes sites favorable for HBD solvent interactions. As can be seen from the MEP map of the molecules, negative regions are mainly localized over the carbonyl groups from the TZD moiety and over the *nitro* and *metoxy* substituents in the compounds **1h**, **1i**, **2g** and **2i** (Figs. S13 and S14). The positive region is localized on the methyl and phenyl groups attached on nitrogen atom in TZD moiety. This effect is the least pronounced in molecules **1g** and **2g** with strong electron-donating *dimethylamino* substituent is present at phenyl ring causing shifting electronic density to electro-accepting TZD ring. Most of HBA capabilities of TZD molecules could be assumed to be from *2,4-dioxo* groups as strong electron-acceptor groups that cause increase in electron density at these two sites creating favorable interaction with proton-donating solvents. As can be seen from the MEP map of the compounds, the regions having the negative potential are over the electronegative atoms, the regions having the positive potential are over the *methyl* and *phenyl* groups attached to nitrogen atom and the remaining species are surrounded by zero potential.

The experimental and theoretical study implies that the solvatochromic properties are the consequence of the overall effect of the molecule geometry influenced by the electronic substituent effects transmitted through π-conjugated systems and results obtained in this study help in assessing the potential application of the investigated compounds in different homogeneous media.

4. Conclusions

The substituent and solvent effects on the UV–vis absorption maxima shifts of TZDs were successfully evaluated from the results of LSER and LFER correlation analysis. Solvent polarizability is the principal factor influencing the bathochromic shift of absorption maxima indicating that the excitation state is more polarizable than the ground state. Specific interactions through hydrogen bonding were attributed to the carbonyl groups in TZD moiety, and these interactions were slightly affected by the substituent present in arylidene part. The LFER correlations results obtained separately for electron-donating and electron-accepting substituents reflect different transmission modes of electronic substituent effects through differently oriented π-electronic units.

The LFER analysis appears to be a straightforward method for correlations of *SCS* values with the appropriate substituent constants. The π-polarization concept, including localized and extended π-polarization, has aided in explaining successfully the normal and reverse substituent effect at C5 and C6 atoms, respectively. The comparative analysis of the correlation results for series **1** and **2** with those obtained for eight structurally related styrene series has indicated that specific electronic cross-interaction of substituent and heterocyclic moieties contributed to electronic density shift.

Additionally MP2 calculations showed that optimized geometries of investigated compounds showed that substituent induces low decrease in torsion angle (θ). Strong electron-donor (*metoxy* and *dimethylamino*) substituent supports an electron density shift from the π_1-unit to the electron-accepting TZD moiety contributing to more planar conformation, while larger deviation was found in electron-acceptor substituted compounds.

Calculation of the HOMO–LUMO energy gaps contributed to understanding the mechanism of electronic excitations. Unsubstituted compounds have the largest energy gaps of 6.582 eV (**1a**) and 6.542 eV (**2a**), while the lowest energy gaps were found for compounds **1g** and **2g** with 5.776 and 5.727 eV, respectively, which is consistent with their largest bathochromic shift. Variation of substituent patterns clearly indicates that contributions of both structural and donor-acceptor character of studied molecule are involved in the ICT mechanism of the investigated molecules.

TD-DFT calculations were additionally performed to define the D_{CT}, Q_{CT} and μ_{CT} of studied TZDs. Obtained results indicate that the strongest ICT was found for **1g** and **2g** molecules, *i.e. dimethylamino* substituted compound, with transfer of 0.567 e^- over 2.939 Å and 0.566 e^- over 2.980 Å, respectively. On the other hand, in compounds **1h** and **2h**, i.e. *nitro* substituted compounds, intramolecular charge transfer of 0.737 e^- over 0.989 Å and 0.736 e^- over 0.988 Å, respectively, represent a local process which occurs within *nitro* substituent.

Acknowledgments

This work was supported by the Ministry of Education, Science and Technological Development of Serbia (Project Number 172013).

Appendix A. Supplementary material

Supplementary data associated with this article can be found, in the online version, at http://dx.doi.org/10.1016/j.arabjc.2016.12.013.

References

Abbehausen, C., de Paiva, R.E.F., Formiga, A.L.B., Corbi, P.P., 2012. Studies of the tautomeric equilibrium of 1,3-thiazolidine-2-thione: theoretical and experimental approaches. Chem. Phys. 408, 62–68.

Azam, F., Prasad, M.V., Thangavel, V., 2012. Targeting oxidative stress component in the therapeutics of epilepsy. Curr. Top. Med. Chem. 12, 994–1007.

Barany, J.M., Hammer, R.P., Merrifield, R.B., Barany, G., 2005. Efficient synthesis of 1,2,4-dithiazolidine-3,5-diones [dithiasuccinoyl-amines] from bis(chlorocarbonyl)- disulfane plus Bis (trimethylsilyl)amines. J. Am. Chem. Soc. 127, 508–509.

Bharatam, P.V., Khanna, S., 2004. Rapid racemization in thiazolidinediones: a quantum chemical study. J. Phys. Chem. A 108, 3784–3788.

Brown, F.C., 1961. 4-Thiazolidinones. Chem. Rev. 61, 463–521.

Casale, T.B., Stokes, J.R., 2008. Immunomodulators for allergic respiratory disorders. J. Allergy Clin. Immunol. 121, 288–296.

Catalán, J., 2009. Toward a generalized treatment of the solvent effect based on four empirical scales: dipolarity (SdP, a new scale), polarizability (SP), acidity (SA), and basicity (SB) of the medium. J. Phys. Chem. B 113, 5951–5960.

Chandrappa, S., Benaka Prasad, S.B., Vinaya, K., Ananda Kumar, C. S., Thimmegowda, N.R., Rangappa, K.S., 2008. Synthesis and in vitro antiproliferative activity against human cancer cell lines of novel 5-(4-methyl-benzylidene)-thiazolidine-2,4-diones. Invest. New Drugs 26, 437–444.

Chen, L., Thompson, T.R., Hammer, R.P., Barany, G., 1996. Synthetic, mechanistic, and structural studies related to 1,2,4-dithiazolidine-3,5-dione. J. Org. Chem. 61, 6639–6645.

Ciofini, I., Le Bahers, T., Adamo, C., Odobel, F., Jacquemin, D., 2012. Through-space charge transfer in rod-like molecules: lessons from theory. J. Phys. Chem. C 116, 11946–11955.

Cornelis, A., Lambert, S., Laszlo, P., Schaus, P., 1981. Analysis of carbon-13 nuclear magnetic resonance shifts in terms of substituent parameters: statistical comparison of dual and single substituent parameter treatments. J. Org. Chem. 46, 2130–2134.

Craik, D.J., Brownlee, R.T.C., Sadek, M., 1982. Transmission of substituent effects via molecular lines of force: defense of the DSP method and an illustration of its use in explaining π-polarization. J. Org. Chem. 47, 657–661.

Craik, D.J., Brownlee, R.T.C., 1983. Substituent effects on chemical shifts in the sidechains of aromatic systems. Prog. Phys. Org. Chem. 14, 1–73.

Enchev, V., Petkov, I., Chorbadijev, S., 2002. Comparative study of the structure of rhodanine, isorhodanine, thiazolidine-2,4-dione, and thiorhodanine. Chem. Heterocycl. Comp. 38, 1110–1120.

Hamer, G.K., Peat, I.R., Reynolds, W.F., 1973a. Investigations of substituent effects by nuclear magnetic resonance spectroscopy and all-valence electron molecular orbital calculations. I. 4-substituted styrenes. Can. J. Chem. 51, 897–913. Can. J. Chem. 5, 897–914.

Hamer, G.K., Peat, I.R., Reynolds, W.F., 1973b. Investigations of substituent effects by nuclear magnetic resonance spectroscopy and all-valence electron molecular orbital calculations. II. 4-substituted α-methylstyrenes and α-t-buthylstyrenes. Can. J. Chem. 51, 915–926.

Hansch, C., Leo, A., Hoekman, D., 1995. Exploring QSAR: hydrophobic, electronic and steric constants. American Chemical Society, ACS Professional Reference Book, American Chemical Society, Washington, DC.

Heidi, S.C., 2003. Thiazolidinediones in diabetes: current status and future outlook. Curr. Opin. Invest. Drugs 4, 406–411.

Hilal, R., Osman, A., 1978. A molecular orbital treatment of the electronic structure and spectra of tautomeric rhodanines. Appl. Spectr. 32, 557–563.

Huang, J.W., Shiau, C.W., Yang, Y.T., Kulp, S.K., Chen, K.F., Brueggemeier, R.W., Shapiro, C.L., Chen, C.S., 2005. Peroxisome proliferator-activated receptor gamma-independent ablation of cyclin D1 by thiazolidinediones and their derivatives in breast cancer cells. Mol. Pharmacol. 67, 1342–1348.

Jacquemin, D., Le Bahers, T., Adamo, C., Ciofini, I., 2012. What is the "best" atomic charge model to describe through-space charge-transfer excitations? Phys. Chem. Chem. Phys. 14, 5383–5388.

Jain, R., Bally, T., Rablen, P.R., 2009. Calculating accurate proton chemical shifts of organic molecules with density functional methods and modest basis sets. J. Org. Chem. 74, 4017–4023.

Kamlet, M.J., Abbound, J.L.M., Taft, R.W., 1981. An examination of linear solvation energy relationships. In: Taft, R.W. (Ed.), . In: Progress in Physical Organic Chemistry, vol. 13. Wiley, New York, pp. 485–630.

Kim, K.Y., Kim, S.S., Cheon, H.G., 2006. Differential anti-proliferative actions of peroxisome proliferator-activated receptor-gamma agonists in MCF-7 breast cancer cells. Biochem. Pharmacol. 72, 530–540.

Krabbenhoft, H., 1978. Correlation of σ^+ and σ^- substituent constants with carbon-13 shieldings of β-carbons of para-Substituted β, β-dichlorostyrenes. J. Org. Chem. 43, 1830–1832.

Le Bahers, T., Adamo, C., Ciofini, I., 2011. A qualitative index of spatial extent in charge-transfer excitations. J. Chem. Theor. Comput. 7, 2498–2506.

Macháček, V., Štěrba, V., Zahradníčková, H., 1981. Solvolysis kinetics and mechanism of 3-methyl-1,3-thiazolidine-2,4-dione. Collect. Czech. Chem. Commun. 46, 3097–3103.

Lestard, M.E.D., Gil, D.M., Estevez-Hernandez, O., Erben, M.F., Duque, J., 2015. Structural, vibrational and electronic characterization of 1-benzyl-3-furoyl-1-phenylthiourea: an experimental and theoretical study. New J. Chem. 39, 7459–7471.

Luo, Y., Ma, L., Zheng, H., Chen, L., Li, R., He, C., Yang, S., Ye, X., Chen, Z., Li, Z., Gao, Y., Han, J., He, G., Yang, L., Wei, Y., 2010. Discovery of (Z)-5-(4-methoxybenzylidene)thiazolidine-2,4-dione, a readily available and orally active glitazone for the treatment of concanavalin A-induced acute liver injury of BALB/c mice. J. Med. Chem. 53, 273–381.

Ma, L.A., Xie, C.F., Ma, Y.H., Liu, J.A., Xiang, M.L., Ye, X., Zheng, H., Chen, Z.Z., Xu, Q.Y., Chen, T., Chen, J.Y., Yang, J.C., Qiu, N., Wang, G.C., Liang, X.L., Peng, A.H., Yang, S.Y., Wei, Y.Q., Chen, L.J., 2011. Synthesis and biological evaluation of novel 5-benzylidenethiazolidine-2,4-dione derivatives for the treatment of inflammatory diseases. J. Med. Chem. 54, 2060–2068.

Maltarollo, V.G., Homem-de-Mello, P., Honório, K.M., 2010. Theoretical study on the molecular and electronic properties of some substances used for diabetes mellitus treatment. J. Mol. Model. 16, 799–804.

Marković, R., Shirazi, A., Džambaski, Z., Baranac, M., Minić, D., 2004. Configurational isomerization of push-pull thiazoliclinone derivatives controlled by intermolecular and-intramolecular RAHB: H-1 NMR dynamic investigation of concentration and temperature effects. J. Phys. Org. Chem. 17, 118–123.

Mendgen, T., Steuer, C., Klein, C.D., 2012. Privileged scaffolds or promiscuous binders: a comparative study on rhodanines and related heterocycles in medicinal chemistry. J. Med. Chem. 55, 743–753.

Oakes, N.D., Kennedy, C.J., Jenkins, A.B., Ross-Laybutt, D., Chisholm, D.J., Kraegen, E.W., 1994. A new antidiabetic agent, BRL 49653, reduces lipid availability and improves insulin action and glucoregulation in the rat. Diabetes 43, 1203–1210.

Rančić, M., Trišović, N., Milčić, M., Uščumlić, G., Marinković, A., 2012. Substituent and solvent effects on intramolecular charge transfer of 5-arylidene-2,4-thiazolidinediones. Spectrochim. Acta A 86, 500–507.

Rančić, M., Trišović, N., Milčić, M., Ajaj, I., Marinković, A., 2013. Experimental and theoretical study of substituent effect on 13C NMR chemical shifts of 5- arylidene-2,4-thiazolidinediones. J. Mol. Struct. 1049, 59–68.

Rekha, S., Shanthram, U., Vineet, C., 2011. Synthesis and evaluation of novel thiazolidinediones for antiinflammatory activity. 2011. IRJP 2, 81–84.

Roux, M.V., Temprado, M., Jimenez, P., Foces-Foces, C., Notario, R., 2009. Experimental and theoretical study of the structures and enthalpies of formation of the synthetic reagents 1,3-thiazolidine-2-thione and 1,3-oxazolidine-2-thione. J. Phys. Chem. A 113, 10772–10778.

Saeed, A., Ashraf, S., White, J.M., Soria, D.B., Franca, C.A., Erben, M.F., 2015. Synthesis, X-ray crystal structure, thermal behavior and spectroscopic analysis of 1-(1-naphthoyl)-3-(halo-phenyl)-thioureas complemented with quantum chemical calculations. Spectrochim. Acta A 150, 409–418.

Salamone, S., Colin, C., Grillier-Vuissoz, I., Kuntz, S., Mazerbourg, S., Flament, S., Martin, H., Richert, L., Chapleur, Y., Boisbrun, M., 2012. Synthesis of new troglitazone derivatives: anti-proliferative activity in breast cancer cell lines and preliminary toxicological study. Eur. J. Med. Chem. 51, 206–215.

Sarkar, A., Banerjee, P., Hossain, S.U., Bhattacharya, S., Bhattacharya, S.C., 2009. Role of hydrogen bonding in the spectroscopic properties of thiazolidinedione derivatives in homogeneous solvents. Spectrochim. Acta A 72, 1097–1102.

Singh, S.P., Parmar, S.S., Raman, K., Stenberg, V.I., 1981. Chemistry and biological activity of thiazolidinones. Chem. Rev. 81, 175–203.

Spassova, M., Enchev, V., 2004. Ab initio investigation of the structure and nonlinear optical properties of five-membered heterocycles containing sulfur. Chem. Phys. 298, 29–36.

Romagnoli, R., Baraldi, P.G., Salvador, M.K., Camacho, M.E., Balzarini, J., Bermejo, J., Estévez, F., 2013. Anticancer activity of novel hybrid molecules containing 5-benzylidene thiazolidine-2,4-dione. Eur. J. Med. Chem. 63, 544–557.

Reichardt, C., 2003. Solvents and Solvent Effects in Organic Chemistry. Wiley-VCH, Weinheim.

Reynolds, W.F., Gomes, A., Maron, A., Macintyre, D.W., Tannin, A., Hamer, G.K., Peat, I.R., 1983. Substituent-induced chemical shifts in 3- and 4-substituted styrenes: definition of substituent constants and determination of mechanisms of transmission of substituent effects by iterative multiple linear regression. Can. J. Chem. 61, 2376–2384.

Please cite this article in press as: Rančić, M.P. et al., Solvent and substituent effect on intramolecular charge transfer in 5-arylidene-3-substituted-2,4-thiazolidinediones: Experimental and theoretical study. Arabian Journal of Chemistry (2017), http://dx.doi.org/10.1016/j.arabjc.2016.12.013

Saleh, B.A., Al-Shawi, S.A., Fadhil, G.F., 2008. Substituent effect study on 13Cβ SCS of styrene series. A Yukawa-Tsuno model and Reynolds dual substituent parameter model investigation. J. Phys. Org. Chem. 21, 96–101.

Sortino, M., Delgado, P., Juarez, S., Quiroga, J., Abonia, R., Insuasty, B., Nogueras, M., Rodero, L., Garibotto, F.M., Enriz, R.D., Zacchino, S.A., 2007. Synthesis and antifungal activity of (Z)-5-arylidenerhodanines. Bioorg. Med. Chem. 15, 484–494.

Tan, S.F., Ang, K.P., Fong, Y.F., 1987. Substituent effects in ^{1}H and ^{13}C nuclear magnetic resonance correlations of chemical shifts in para-substituted 5-arylmethylenehydantoins. J. Chem. Soc. Perkin. Trans. 2, 1043–1045.

Tan, S.F., Ang, K.P., How, G.F., 1990. NMR spectroscopic study of configurations and conformations of 5-pyridylmethylenehydantoins. J. Phys. Org. Chem. 3, 559–566.

Tomašić, T., Zidar, N., Mueller-Premru, M., Kikelj, D., Peterlin Masic, L., 2010. Synthesis and antibacterial activity of 5-ylidenethiazolidin-4-ones and 5-benzylidene-4,6-pyrimidinediones. Eur. J. Med. Chem. 45, 1667–1672.

Tomašić, T., Peterlin Masic, L., 2009. Rhodanine as a privileged scaffold in drug discovery. Curr. Pharm. Des. 16, 1596–1629.

Uchiyama, S., Ando, M., Aoyagi, S., 2003. Isomerization of aldehyde-2,4-dinitrophenyl hydrazone derivatives and validation of high-performance liquid chromatographic analysis. J. Chromatogr. A 996, 95–102.

Wiesenberg, I., Chiesi, M., Missbach, M., Spanka, C., Pignat, W., Carlberg, C., 1998. Specific activation of the nuclear receptors PPAR and RORA by the antidiabetic thiazolidinedione BRL 49653 and the antiarthritic thiazolidinedione derivative CGP 52608. Mol. Pharmacol. 53, 1131–1138.

Zvarec, O., Polyak, S.W., Tieu, W., Kuan, K., Dai, H., Pedersen, D.S., Morona, R., Zhang, L., Booker, G.W., Abell, A.D., 2012. 5-Benzylidenerhodanine and 5-benzylidene-2-4-thiazolidinedione based antibacterials. Bioorg. Med. Chem. Lett. 22, 2720–2722.

Yamin, B.M., Yusof, M.S.M., 2003. N-benzoyl-N'-phenylthiourea. Acta Cryst. E 59, 151–152.

Yang, D.-H., Yang, B.-Y., Chen, Z.-C., Chen, S.-Y., Zheng, Q., 2005. Organic reaction in ionic liquids: ionic liquid-accelerated facile synthesis of 3-alkyl-2,4-thiazolidinediones. J. Chem. Res., 492–494

Yang, D.-H., Gao, H.-L., Yang, B.-Y., Chen, Z.-C., 2008. Ionic liquid-accelerated N-arylation of 5-arylidene-2,4-thiazolidinediones with diaryliodonium salts. J. Chem. Res. 12, 686–687.

Please cite this article in press as: Rančić, M.P. et al., Solvent and substituent effect on intramolecular charge transfer in 5-arylidene-3-substituted-2,4-thiazolidinediones: Experimental and theoretical study. Arabian Journal of Chemistry (2017), http://dx.doi.org/10.1016/j.arabjc.2016.12.013